PRODUCTION OF FLAME RETARDANT POLYESTER COMPOSITES AND FIBERS

A THESIS SUBMITTED TO
THE GRADUATE SCHOOL OF NATURAL AND APPLIED SCIENCES
OF
MIDDLE EAST TECHNICAL UNIVERSITY

BY

MİTHAT AKAN

IN PARTIAL FULFILLMENT OF THE REQUIREMENTS
FOR
THE DEGREE OF MASTER OF SCIENCE
IN
POLYMER SCIENCE AND TECHNOLOGY

SEPTEMBER 2013

Approval of the thesis:

PRODUCTION OF FLAME RETARDANT POLYESTER COMPOSITES AND FIBERS

submitted by **MITHAT AKAN** in partial fulfillment of the requirements for the degree of **Master of Science in Polymer Science and Technology Department, Middle East Technical University** by,

Prof. Dr. Canan Özgen _____
Dean, Graduate School of **Natural and Applied Sciences**

Prof. Dr. Teoman Tinçer _____
Head of Department, **Polymer Science and Technology**

Prof. Dr. Erdal Bayramlı _____
Supervisor, **Chemistry Dept., METU**

Prof. Dr. Göknur Bayram _____
Co-Supervisor, **Chemical Engineering Dept., METU**

Examining Committee Members:

Prof. Dr. Jale Hacaloğlu _____
Chemistry Dept., METU

Prof. Dr. Erdal Bayramlı _____
Chemistry Dept., METU

Prof. Dr. Göknur Bayram _____
Chemical Engineering Dept., METU

Prof. Dr. Ceyhan Kayran _____
Chemistry Dept., METU

Assist. Prof. Dr. Akın Akdağ _____
Chemistry Dept., METU

Date: 04.09.2013

I hereby declare that all information in this document has been obtained and presented in accordance with academic rules and ethical conduct. I also declare that, as required by these rules and conduct, I have fully cited and referenced all material and results that are not original to this work.

Name, Last name: Mithat AKAN

Signature

ABSTRACT

PRODUCTION OF FLAME RETARDANT POLYESTER COMPOSITES AND FIBERS

Akan, Mithat

M.S., Department of Polymer Science and Technology

Supervisor: Prof. Dr. Erdal Bayramlı

Co-supervisor: Prof. Dr. Göknur Bayram

September 2013, 51 Pages

Poly(ethylene terephthalate) (PET) fiber is one of the leading synthetic fibers in textile industry. However, its flame retardant properties are poor to be used in certain applications, therefore flame retardant additives are generally used in order to improve flame retardant properties of PET.

The main objective of this study is to find suitable flame retardant additives for PET that can synergize with each other and that can improve the flame retardant properties without compromising the mechanical properties of PET.

PET fibers were prepared by using a twin screw micro-compounder at 260 ºC and 100 rpm for 3 minutes.

Main flame retardant additive of the study is zinc phosphinate. Nano-zinc borate and huntite-hydromagnesite were used as synergists to increase the flame retardant and mechanical properties of PET. 10% zinc phosphinate and 2% and 4% synergists were mixed with PET and tested for mechanical and flame retardant properties.

Test results show that zinc phosphinate-zinc borate system, while providing sufficient flame retardant properties, led to poor tensile strength. On the other hand, PET with zinc phosphinate and huntite-hydromagnesite has both sufficient flame retardant properties and better mechanical properties than PET with zinc phosphinate and zinc borate. As a result, zinc phoshinate-huntite-hydromagnesite system can be suggested to improve the flame retardant properties of PET.

Keywords: PET, synergism, zinc phosphinate, flame retardancy

ÖZ

ALEV GECİKTİRİCİLİ POLYESTER KOMPOZİTLERİNİN VE ELYAFLARININ ÜRETİMİ

Akan, Mithat

Yüksek Lisans, Polimer Bilimi ve Teknolojisi Bölümü

Tez Yürütücüsü: Prof. Dr. Erdal Bayramlı

Ortak Tez Yürütücüsü: Prof. Dr. Göknur Bayram

Eylül 2013, 51 Sayfa

Poly(ethylene terephthalate) (PET) tekstil endüstrisinin önde gelen sentetik elyaflarından biridir. Ancak PET'in alev geciktirici özellikleri belli uygulamalarda kullanılabilmek için zayıftır, bu yüzden PET'in alev geciktirici özelliklerini iyileştirme amacıyla genellikle alev geciktiricili katkı maddesi kullanılır.

Bu çalışmanın temel amacı; birbirleriyle sinerji yapabilen ve PET'in mekanik özelliklerini düşürmeden alev geciktirici özelliklerini arttıran, PET'e uygun alev geciktiricili katkı maddeleri bulmaktır.

PET elyafları çift vidalı mikro karıştırıcı kullanarak 260 ºC ve 100 rpm'de 3 dakika karıştırılarak hazırlandı.

Bu çalışmanın ana katkı maddesi çinko fosfinat'dır. PET'in mekanik ve alev geciktirici özelliklerini arttırmak için nano-çinko borat ve huntit-hidromagnezit sinerjist olarak kullanıldı. %10 çinko fosfinat ve %2 ve %4 sinerjist malzeme PET ile karıştırıldı ve mekanik ve alev geciktirici özellikleri için test edildi.

Test sonuçlarına göre, çinko fosfinat-çinko borat sistemi yeterli alev geciktirici özellikler gösterse de düşük çekme dayanımına sebep oldu. Öte yandan çinko fosfinat'lı ve huntit-hidromagnezit'li PET hem yeterli alev geciktirici özelliğine hem de çinko fosfinat'lı ve çinko borat'lı PET'ten daha iyi mekanik özelliklere sahiptir. Sonuç olarak, çinko fosfinat-huntit-hidromagnezit PET'in alev geciktirici özelliğini arttırmak için önerilebilir.

Anahtar Kelimeler: PET, sinerjizm, çinko fosfinat, alev geciktiricilik

To my family

ACKNOWLEDGEMENTS

I would like to express my deepest gratitude to my thesis supervisor Prof. Dr. Erdal Bayramlı for his guidance, understanding, kind support, encouraging advices, criticism, and valuable discussions throughout my thesis.

I am greatly indebted to Prof. Dr. Göknur Bayram from Department of Chemical Engineering for her guidance.

I wish to thank Yağmur Özaltan for her patient love and for not leaving me alone in my stressful days.

I would like to sincerely thank Ümit Tayfun and Selahattin Erdoğan for their friendship and help.

I dedicate this dissertation to each and every member of my family who always offered their advice, love, care and support. My family's absolute unquestionable belief in me, have been a constant source of encouragement and have helped me achieve my goals.

TABLE OF CONTENTS

ABSTRACT…….. v

ÖZ……..... vii

ACKNOWLEDGEMENTS…….. x

TABLE OF CONTENTS……..…… xi

LIST OF TABLES…… xi

LIST OF FIGURES…...…….….. xii

LIST OF ABBREVIATIONS…...…….. xiv

CHAPTERS

1. INTRODUCTION 1
2. BACKGROUND INFORMATION 3
   - 2.1 Properties of Poly(ethylene terephthalate) 3
   - 2.2 Flame Retardant Additives 3
     - 2.2.1 Phosphorus Based Flame Retardants 4
     - 2.2.2 Zinc Borate 5
     - 2.2.3 Mineral Flame Retardant Additives 6
     - 2.2.4 Flame Retardancy in Synthetic Fiber and Fabrics 8
   - 2.3 Flame Retardancy Mechanism 9
   - 2.4 Characterization Tests 10
     - 2.4.1 Mechanical Test 10
       - 2.4.1.1 Tensile Test 10
     - 2.4.2 Flame Retardancy Test 12
       - 2.4.2.1 Limiting Oxygen Index 12
     - 2.4.3 Scanning Electron Microscopy (SEM) 12
   - 2.5 Previous Studies 12
3. EXPERIMENTAL WORK 15
   - 3.1 Materials 15
   - 3.2 Sample Preparation 16

3.2.1 Extrusion 16
3.2.2 Drying 17
3.2.3 Samples 17
3.3 Tensile Tests 18
3.3.1 Standard Test Method for Tensile Properties of Plastics (ASTM D638-03) 18
3.3.2 Standard Test Method for Tensile Strength and Young's Modulus of Fibers (ASTM C1557) 20
3.4 Flammability Tests 21
3.5 Wide Angle X-ray Scattering (WAXS) 23
3.6 Scanning Electron Microscopy (SEM) Analysis 23
4. RESULTS & DISCUSSION 25
4.1 Mechanical and Flame Retardant Properties 25
4.1.1 PET with Zinc Phosphinate (ZnPi) 25
4.1.2 Zinc Borate as a Synergy Agent 30
4.1.3 Adding Surface Treated Zinc Borate 32
4.1.4 Huntite Hydromagnesite as a Synergist 33
4.2 Morphological Analysis 35
5. CONCLUSION 43
REFERENCES 45

LIST OF TABLES

TABLES

Table 2.1 Environmental Advantages and disadvantages of Phosphorus based flame retardants 4
Table 2.2 Mechanisms of action of zinc borate on different polymer matrices 6
Table 3.1 Properties of Exolit OP 950 15
Table 3.2 Chemical composition of huntite-hydromagnesite 16
Table 3.3 Properties of huntite-hydromagnesite 16
Table 3.4 Specification of Xplore Micro-Compounder 17
Table 3.5 Percentages and labels of all PET samples that were prepared in this study 18
Table 4.1 Samples with different percentages of Zinc phosphinate and PET 25
Table 4.2 Properties Tensile strength, maximum elongation and LOI values for OP0, 5, 10, 15, 20 26
Table 4.3 Crystalline and amorphous area of the WAXS from Figure 4.2 and % crystallinity 30
Table 4.4 Samples with percentages of Zinc phosphinate, zinc borate and PET 30
Table 4.5 Mechanical properties and LOI values for OP0, OP10, and OP10ZnB2 31
Table 4.6 Samples with percentages of PET, zinc phosphinate and the two types of zinc borate 32
Table 4.7 Mechanical and LOI values for surface treated nano-ZnB-PET fibers 33
Table 4.8 Samples with percentages of PET, ZnPi and huntite-hydromagnesite 34
Table 4.9 Mechanical and LOI values of PET samples with both zinc phosphinate and huntite-hydromagnesite as the synergist 35
Table 4.10 EDX analysis of the fiber surface of the PET sample 2% ZnB and 10% ZnPi . 38
Table 4.11 EDX analysis of the stretched area on PET sample with 2% treated-ZnB and 10% ZnPi 40
Table 4.12 EDX analysis of the PET sample with 2% huntite-hydromagnesite and 10% ZnPi 42

LIST OF FIGURES

FIGURES

Figure 2.1 Structure of PET 3
Figure 2.2 Total FR consumption in Europe in 2006, estimated to be 465.000 tonnes 5
Figure 2.3 Scanning electron microscope (SEM) graph of huntite-hydromagnesite 8
Figure 2.4 Stress vs. strain graph of a typical polymer during a tensile test 11
Figure 2.5 Dog-bone shape (Upper part) and single fiber (Lower part) specimen for ASTM D638-03 and ASTM C1557 11
Figure 3.1 Chemical formula of zinc phosphinate compound 15
Figure 3.2 Twin screw micro compounder (DSM Xplore) 17
Figure 3.3 Tensile testing machine (Lloyd) 18
Figure 3.4 Injection molding machine 19
Figure 3.5 View of the dog-bone mold in the injection molding machine 19
Figure 3.6 Dimensions for dog-bone mold 20
Figure 3.7 DSM Xplore Microfiber spin line 20
Figure 3.8 Limiting oxygen index machine 21
Figure 3.9 Dimensions for LOI test sample 21
Figure 3.10 Compression molding machine 22
Figure 3.11 Horizontal and vertical layers for woven-mat LOI sample 23
Figure 4.1 Tensile strength vs. percentage strain of OP0, OP5, OP10, OP15, OP20 dog-bone samples 26
Figure 4.2 WAXS intensity vs. 2theta for the samples OP0, OP5, OP10, OP15 and OP20 with baselines 27
Figure 4.2 (cont'd) WAXS intensity vs. 2theta for the samples OP0, OP5, OP10, OP15 and OP20 with baselines 28
Figure 4.2a WAXS intensity vs. 2theta graph of 100% ZnPi sample 29
Figure 4.3 Stress vs. Strain curve for PET only, OP10 and OP10ZnB2 fiber samples 31

Figure 4.4 Stress vs. strain curves for OP0, OP10, OP10ZnB2, 10% OP +surface treated 2% ZnBs (OP10T-ZnB) and 10% OP + batch mix 2% ZnB (OP10BM-ZnB2) 32
Figure 4.5 Stress vs. strain curve for OP10HH2, OP10HH4 and OP0HH10 for fiber samples 34
Figure 4.6a Chemical SEM micrograph of a pure PET sample 36
Figure 4.6b SEM micrograph of PET showing the deformations on the surface 36
Figure 4.7a SEM micrograph of PET with 2% ZnB and 10% ZnPi sample 37
Figure 4.7b SEM micrograph of a fiber on the same PET sample with 2% ZnB and 10% ZnPi 38
Figure 4.8a SEM micrograph of stretch area of PET sample with 2% treated-ZnB and 10% ZnPi 39
Figure 4.8b SEM micrograph of fractured end of the PET sample with 2% treated-ZnB and 10% ZnPi 39
Figure 4.8c SEM micrograph of the other end of the PET sample with 2% treated-ZnB and 10% ZnPi 40
Figure 4.9a SEM micrograph of PET sample with 2%n huntite-hydromagnesite and 10% ZnPi 41
Figure 4.9b One of the fractured ends of same PET sample with 2% huntite-hydromagnesite and 10% ZnPi 41
Figure 4.9c The other fractured end of the PET sample with 2% huntite-hydromagnesite and 10% ZnPi 42

LIST OF ABBREVIATIONS

PET	Poly(ethylene terephthalate)
ZnPi,OP	Zinc phosphinate
ZnB	Zinc borate
LOI	Limiting Oxygen Index
PFR	Phosphorus based Flame Retardants
HH	Huntite-hydromagnesite
WAXS	Wide angle X-ray scattering
SEM	Scanning electron microscopy

CHAPTER 1

INTRODUCTION

Poly(ethylene terephthalate) (PET), the third most produced polymer, with its good mechanical properties (high tensile strength and elasticity), good chemical properties and low cost have found many applications. The foremost usage for PET is in textile industry, in which PET is the leading synthetic fiber.

However, its thermal stability at high temperatures is poor and dripping effect occurs, which can lead to fabrics and clothes becoming a fire hazard, therefore many studies were performed to improve flame retardancy of this polymer [1-7].

There are a number of ways to achieve high flame retardancy for the polymers [8, 9]:

a) Polymers that have high resistance to fire themselves,
b) Chemical modification: e.g. copolymerization with flame retardant monomers,
c) Using melt blending to introduce flame retardant additives,
d) Application of flame retardant to the surface of a fabric to delay burning.

Although all of the methods have seen some use, such as copolymerization with flame retardant monomers [10-12] and melt blending [13, 14], melt blending comes forward due to the flexibility of the method; additives can be easily introduced into the polymer. However, a limitation is that the additive should not degrade in the processing temperature of the polymer which, in the case of PET, is around 260 ºC.

Another limitation to consider is that adding high percentages of flame retardant may affect other properties such as mechanical properties [15, 16]. To counter this, employing synergism is an effective way. Synergism occurs when two flame retardants interact positively to make a higher effect on the flame retardancy of the polymer than the sum of both flame retardants [17, 18]. Using two different flame retardants with synergistic effect in smaller amounts will give one either the same or better flame retardancy without compromising mechanical properties of the polymer.

A flame retardant group of this study to use with PET is phosphinates. The allure of phosphorus-containing additives comes from being halogen-free additives. Shaw et al. [19] concluded in their review that halogenated flame retardants cause health and environmental problems. Therefore, studies have turned to halogen-free flame retardants [20, 21]. These types of additives act mostly through forming a condensed phase. Char formation on the surface during the combustion is an example of this phenomenon.

One type of flame retardant that can be used for synergism is nanoparticles which are particles with at least one dimension in the nano-region (<100 nm) [22, 23]. Since nanoparticles have large surface area, they may interact with the polymer in a high extent; therefore, even in small amounts they should greatly improve the flame retardancy of the polymer. Nanoparticles generally form a protective layer during combustion which reduces the interaction between the polymer and air. Polyhedral oligomeric silsesquioxanes (POSS) ([24-27]) and nanoclays [28] are examples for nanoparticles that improve the flame retardancy of polymers.

Huntite-hydromagnesite is a mixture of minerals and it is another type of flame retardant that can improve the flame retardant property of PET. Huntite is a magnesite carbonate mineral while hydromagnesite is a hydrated magnesite carbonate mineral. Huntite-hydromagnesite works as a flame retardant by decomposing into water and carbon dioxide gas which interferes with the decomposition of PET. About 54% mass of huntite-hydromagnesite turns into water and CO_2 during decomposition [29].

The aim of this study is to investigate the possible synergistic effects among different inorganic powders such as nano-zinc borate and huntite-hydromagnesite and zinc phosphinate in order to improve the flame retarding properties of PET fibers. Mechanical properties of produced PET samples containing different inorganic powders were measured by means of tensile tests. Limiting oxygen index measurements were used to assess the flame retardant properties of the samples. Dispersion of the additives and the structure of the composites were observed using SEM.

CHAPTER 2

BACKGROUND INFORMATION

2.1 Properties of Poly(ethylene terephthalate)

PET is commonly made by esterification of terephthalic acid and ethylene glycol or transesterification of dimethyl terephthalate and ethylene glycol. The repeating unit of PET is shown in Figure 2.1.

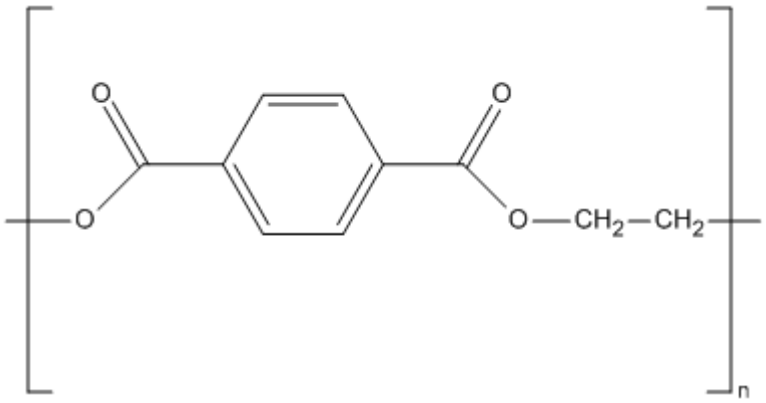

Figure 2.1 – Structure of PET

PET is a thermoplastic polymer having density of 1.3-1.4 g/cm^3 and molecular weight between 20000 and 40000. The thermal properties of PET consist of a melting range between 255 and 265° C. The glass transition temperature, T_g, of PET is in the range of 67 to 81° C [30].

Young modulus of PET is about 3 MPa, and tensile strength is at average 62 MPa. Elongation at break value is between 50-150% [31]. Its impact resistant is high and resistant to repeated stresses. Moreover, since PET has high melting and moderate T_g, it retains good mechanical properties up to 150° C. Its chemical and solvent resistance is also high.

2.2 Flame Retardant Additives

Flame retardants (FRs) are "chemicals which, when added to a combustible material, delay ignition and reduce flame spread of the resulting material when exposed to flame impingement" [32]. It can be noted that no material is fire-proof; all materials burn in a large enough fire. It should also be noted that the tests are generally done in laboratory scales and may not fully represent the behavior of the final product.

2.2.1 Phosphorus Based Flame Retardants

Phosphorus-containing flame retardant additives include but not limited to red phosphorus, phosphates, phosphonates, phosphine oxides and phosphinates. They mainly work by affecting the condensed phase of the polymer combustion[33]. By forming char on the surface of the polymer, it impedes the combustion of a polymer [34]. An example for phosphorus-containing flame retardants (PFRs) is polyurethane foams [35]. Red phosphorus is a system that works both in the condensed and gas phase [35].

PFRs can not only be used with different fiber types in textiles, but also with different processing additives [33]. In addition to this, PFRs are more and more preferred than brominated flame retardants (BFRs) mostly because halogenated flame retardants are bioaccumulative and toxic to the environment. Table 2.1 shows the advantages and disadvantages of PFRs.

Nitrogen-based compounds improve the flame retardancy effect of PFRs depending on the nitrogen compound and the polymer [34, 35]. There are different possibilities for the flame retardant mechanisms of these compounds. One mechanism is that P-N intermediates cause better phosphorylation. Another mechanism is that nitrogen compound decreases the phosphorus released in condensed phase. Third mechanism is that nitrogen enhances the oxidation of phosphorus and therefore releases inert gases, like ammonia [33, 36].

Table 2.1 Advantages and disadvantages of PFRs [37]

Advantages	**Disadvantages**
Effective at low concentrations-organic types of PFRs	Lack of permanency and hygroscopicity of inorganic types of PFRs
Easy incorporation and processing	Potential health hazard during processing organic types of PFRs
Little detrimental effect on physical properties	Release of toxic combustion products from organic types of PFRs
Good UV stability	
Low to moderate prices	

Phosphorus FR made up 20% of total FR consumption in Europe in 2006 (Figure 2.2), estimated to be 465.000 tonnes [38, 39].

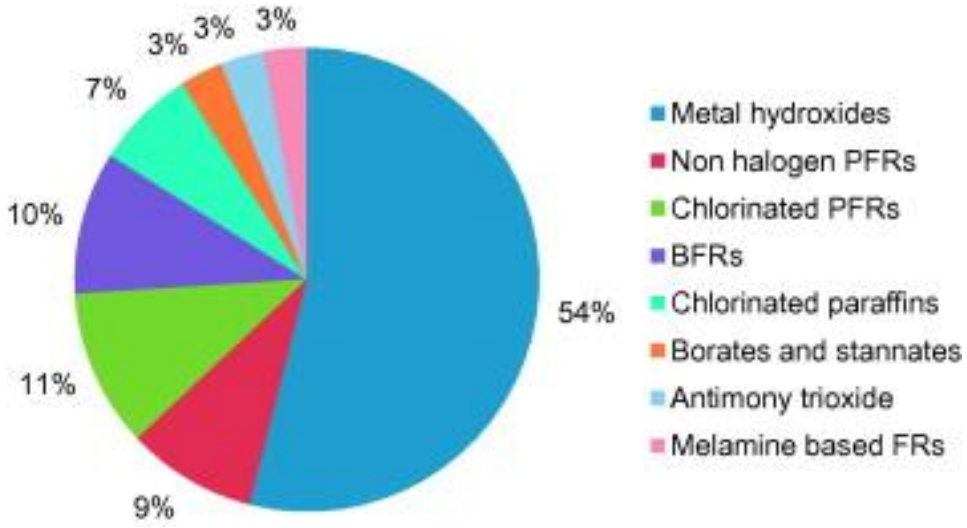

Figure 2.2 – Total FR consumption in Europe in 2006 [37]

2.2.2 Zinc Borate

Zinc borate is an inorganic boron-based flame retardant compound with the general formula of $xZnO \cdot yB_2O_3 \cdot zH_2O$. Even though there exists different chemical formulas such as $ZnO \cdot B_2O_3 \cdot 2H_2O$, $4ZnO \cdot B_2O_3 \cdot H_2O$, $2ZnO \cdot 3B_2O_3 \cdot 7H_2O$, $ZnO \cdot 5B_2O_3 \cdot 4.5H_2O$, $2ZnO \cdot 3B_2O_3 \cdot 3H_2O$, $3ZnO \cdot 5B_2O_3 \cdot 14H_2O$, zinc borate with the formula $2ZnO \cdot 3B_2O_3 \cdot 3.5H_2O$ is the most widely used out of all zinc borate compounds for flame retarding properties [40, 41].

Zinc borate works as a flame retardant additive by releasing the water of hydration at or above 290 °C and B_2O_3 after 350 ° C. This results in a protective char layer formation which prevents gases and heat from interacting with the polymer. Moreover, zinc borate dehydrates endothermically, which means that the hydrated water will absorb the energy generated during combustion and turn into water vapor which will interfere with oxygen-flame interaction [41].

Table 2.2 shows the benefits for different polymer matrices with the addition of zinc borate as a flame retardant. As can be seen from the Table 2.2, it behaves as a char promoter and smoke suppressant for polymer matrices. It also has anti-arcing and anti-tracking agent properties.

Table 2.2 Mechanisms of action of zinc borate on different polymer matrices [40]

Polymer	**Benefit**
PVC	Smoke suppressant Flame retardant Synergist with Sb_2O_3 Lowers total flame retardant cost Char promoter
Polyolefins	Smoke suppressant Char promoter Afterglow suppressant Improves elongation properties Anti-arcing agent
Polyamides	Anti-tracking agent Synergist of halogen sources Afterglow suppressant Used in both halogen containing and halogen-free systems
Elastomers	Smoke suppressant Afterglow suppressant Char promoter Anti-arcing and anti-tracking agent
Epoxy resins	Smoke suppressant Char promoter Partial or completely replace with Sb_2O_3

2.2.3 Mineral Flame Retardant Additives

Mineral FRs constitute the bulk of the FR consumption in the world, with metal hydroxides which is half of the total FR consumption [37]. Among the metal hydroxides, aluminium trihydroxide ($Al(OH)_3$, ATH) and magnesium dihydroxide ($Mg(OH)_2$, MDH) are the most widely known [29].

For metal hydroxides to act as flame retardants, the hydroxyl groups need to undergo endothermic decomposition to produce water. In the case of ATH, this decomposition starts at 220 °C; for MDH, it starts at 330 °C [39]. In addition to endothermicity, a layer of refractory minerals can be used as a heat barrier. A layer of silica was found to decrease the heat released in the absence of catalysis. This is because of poor conduction and reflection of radiant heat becoming a heat-transmission barrier [39,42, 43].

Huntite, a carbonate mineral with the formula of $Mg_3Ca(CO_3)_4$, was first discovered in 1943. It has white color with dull appearance, shows no cleavage and has density of 2.696 [44]. Huntite acts as a flame retardant by the following endothermic decomposition reaction [45-47]:

$$Mg_3Ca(CO_3)_4 \longrightarrow 3\,MgO + 4\,CO_2 + CaO \quad (2\text{-}1)$$

It starts to undergo endothermic decomposition at 450 °C and two decompositions occur; decomposition of huntite to magnesium oxide, carbon dioxide and calcium carbonate, followed by decomposition of calcium carbonate to carbon dioxide and calcium oxide [29].

$$Mg_3Ca(CO_3)_4 \longrightarrow 3\,MgO + CaCO_3 + 3CO_2 \quad (2\text{-}2)$$

$$CaCO_3 \longrightarrow CaO + CO_2 \quad (2\text{-}3)$$

Hydromagnesite is a hydrated carbonate mineral with the formula of $Mg_5(CO_3)_4(OH)_2.4H_2O$, which has endothermic decomposition from 220 °C to 550 °C in 3 steps [29, 48]. First it releases its water of hydration at 220 °C:

$$Mg_5(CO_3)_4(OH)_2 \cdot 4H_2O \longrightarrow Mg_5(CO_3)_4(OH)_2 + 4H_2O \quad (2\text{-}4)$$

then at 330 °C, the hydroxide ion decomposes:

$$Mg_5(CO_3)_4(OH)_2 \longrightarrow Mg_4(CO_3)_4 + MgO + H_2O \quad (2\text{-}5)$$

At 550 °C, carbonate ion decomposes into magnesium oxide and carbon dioxide:

$$Mg_4(CO_3)_4 \longrightarrow 4\,MgO + 4\,CO_2 \quad (2\text{-}6)$$

Figure 2.3 shows the scanning electron microscope (SEM) graph of huntite-hydromagnesite sample. The bigger, blocky particles represent hydromagnesite while the smaller, platy particles represent the huntite.

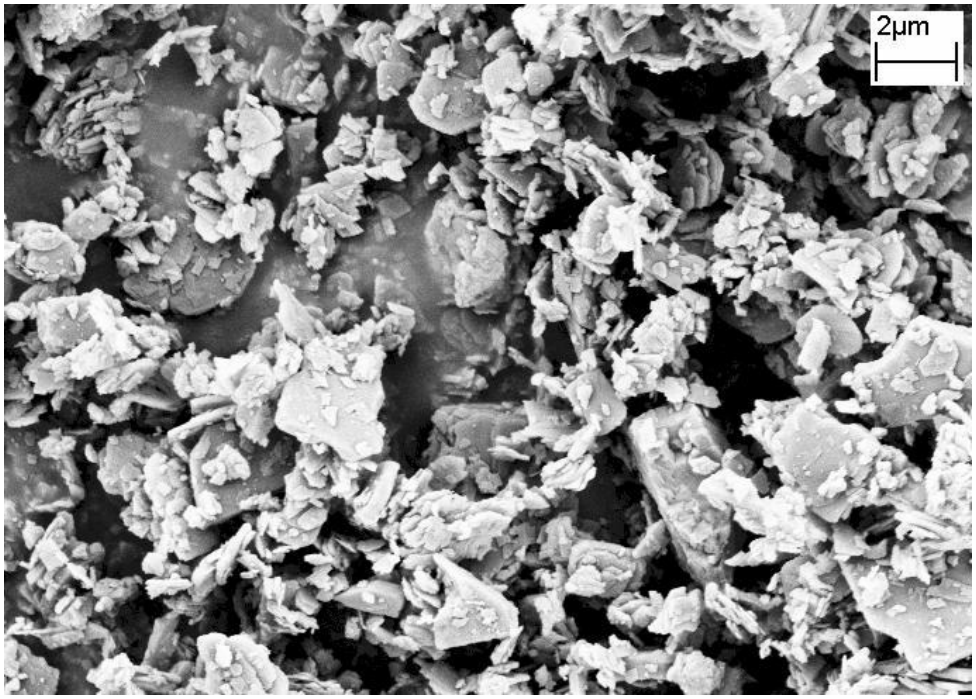

Figure 2.3 – Scanning electron microscope (SEM) graph of huntite-hydromagnesite [29]

2.2.4 Flame Retardancy in Synthetic Fiber and Fabrics

Flame retardancy for textiles started as early as 1735 where mixture of vitriol (metal sulfates), borax (sodium borate), and some mineral substances were patented for flame retardation of canvas [49]. However, what really gave rise to the studies on flame retardancy was during Second World War so as to improve the conditions of the army personnel. After the war, safety legislation concerning the flame retardancy like flame retarded cotton work clothing or children's sleepwear was the driving force [17].

There are three main ways to obtain flame retarded textiles: inherently flame retarded fibers, fibers that were made to be flame retarded during synthesis and chemical after-treatment [50]. Adding flame retardant additives to polymer melt or solution before extrusion is an example to preparing flame retardant fibers [51]. Incorporation of flame retardants into polymer via extrusion has the advantage of being permanent and not easily washed off compared to flame retardancy by surface treatment or surface finishing techniques.
The most common fibers like polyester and nylon are difficult to improve the flame retardancy properties. This is because [50]:

1. Flame retardant additives that are compatible in terms of temperature or do not react with fluid polymers.
2. Flame retardant additive amount necessary to get good flame retardant properties can be high (up to 20% w/w). This cause problem not only in spinning fluid compatibility, but also in mechanical properties necessary for textile fibers.
3. Melt dripping caused by thermoplasticity and melting.

2.3 Flame Retardancy Mechanism

Flame retardant additives are mostly used in improving the flame retardancy of the polymers. There are two mechanisms that flame retardant additives act; through the “gas” or “condensed” phase.

Condensed phase activity involves two different types of reaction. Firstly, flame retardant additive can make an endothermic reaction during combustion which will decrease the temperature and prevent partially the degradation of the polymer. Secondly, protective layer formation can be seen during the combustion. Flame retardant additive can form a layer of residues on top of the polymer, which will suppress both heat and mass transfer between polymer surface and combustion area. These layers can be ceramic-like structure or formed from carbon (char).

Gas phase activity involves mechanism that interferes with gases that are released during combustion. Polymers, during combustion, produce radicals that can react with atmospheric oxygen and cause branching reactions [39]:

$$H\cdot + O_2 \rightarrow OH\cdot + O\cdot \quad (2.7)$$

$$O\cdot + H_2 \rightarrow OH\cdot + H\cdot \quad (2.8)$$

The main reaction that continues to maintain the flame is:

$$OH\cdot + CO \rightarrow CO_2 + H\cdot \quad (2.9)$$

Radicals like O• and OH• can be paired with halogens from halogenated flame retardants and effectively reducing the number of radicals in the combustion area.

In the case of phosphorus-containing FRs, they can operate in condensed or gas phase, sometimes simultaneously in both phases. Phosphorus compounds may form phosphoric or polyphosphoric acids during the combustion. A mechanism for flame retardants with phosphoric acid was suggested in the literature [52]:

$$H_3PO_4 \rightarrow HPO_2 + HPO\cdot + PO\cdot \quad (2.10)$$

$$H\cdot + PO\cdot \rightarrow HPO \quad (2.11)$$

$$HPO + H\cdot \rightarrow H_2 + PO\cdot \quad (2.12)$$

$$PO\cdot + OH\cdot \rightarrow HPO + H_2O \quad (2.13)$$

It can be said that PO · plays a crucial role in the flame retardant mechanism. By reacting with O · and OH · radicals, it will interfere with chain-branching reactions and suppress combustion.

2.4 Characterization Tests

2.4.1 Mechanical Test

Mechanical properties are important as they give an idea about the performance of the material for certain applications. That is to say, mechanical properties such as tensile strength, modulus and elongation at break are needed to be known whether the polymer is suitable for industrial manufacturing or not [53].

2.4.1.1 Tensile Test

Tensile tests measure the force needed to permanently deform a specimen and the extent of elongation at fracture point. ASTM D638-03 and ASTM C1557 can be used for dog-bone shape and fiber samples, respectively.

Cross-sectional area (A_0) and length (l_0) of a specimen are needed to determine the stress (σ) and strain (ε) of the specimen. The relations of these variables are given in the equations below:

$$\sigma = \frac{F}{A_0} \tag{2.14}$$

$$\varepsilon = \frac{l_i - l_0}{l_0} = \frac{\Delta l}{l_0} \tag{2.15}$$

where F is the instantaneous force applied on the specimen and l_i is the instantaneous length. It should be noted that the instantaneous cross-sectional area should be employed to find the actual stress applied to the sample. However, it is customary to use the initial cross-sectional area for convenience. By drawing the stress vs. strain graph of a polymer, maximum tensile strength (highest stress value), Young's modulus (slope of the graph during the elastic deformation) and elongation at break (strain during the rupture point) can be determined. A typical stress vs. strain graph can be seen in Figure 2.4.

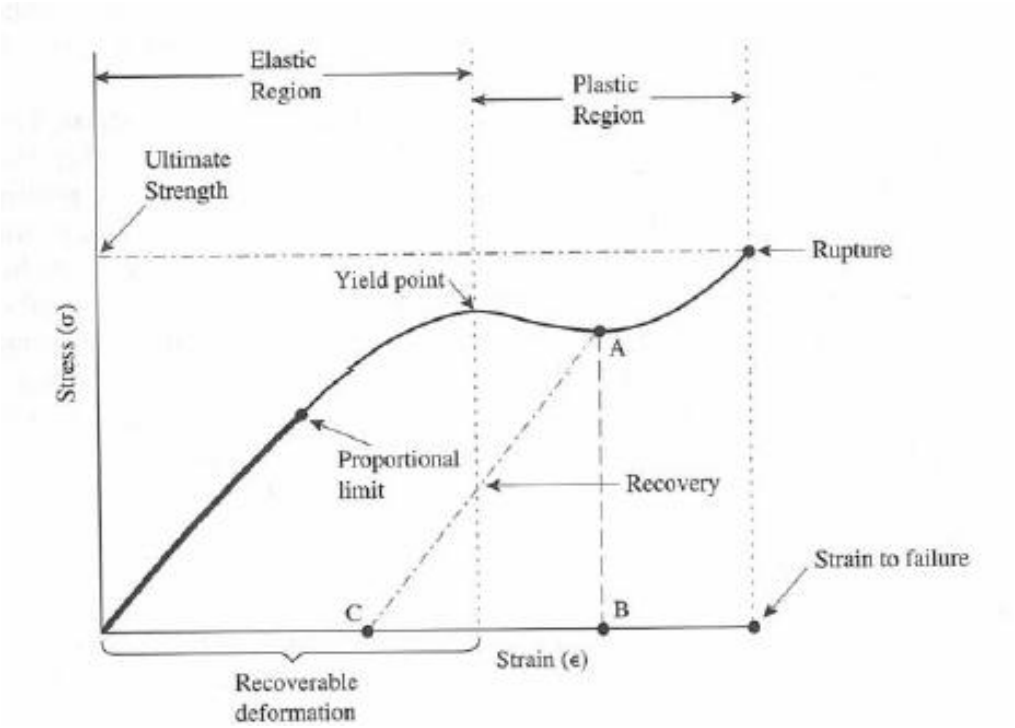

Figure 2.4 – Stress vs. strain graph of a typical polymer during a tensile test [54]

Dimensions of the samples for tensile tests are represented in Figure 2.5.

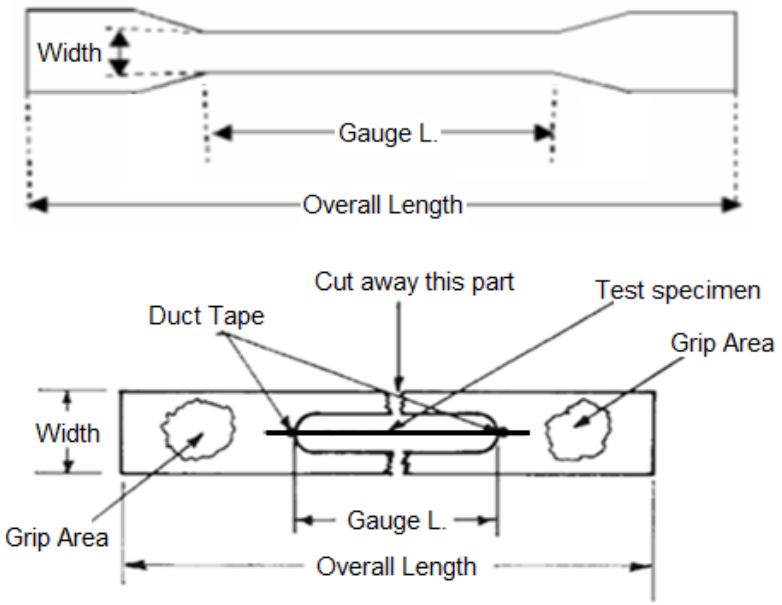

Figure 2.5 – Dog-bone shape (Upper part) and single fiber (Lower part) specimen for ASTM D638-03 and ASTM C1557 [54]

2.4.2 Flame Retardancy Test

2.4.2.1 Limiting Oxygen Index

Limiting Oxygen Index is a commonly used test for flame retardancy in laboratory scale. The specimen is placed in glass chimney and fed continuously with a mixture of nitrogen and oxygen gases. Until the top of the specimen ignites and stable combustion for 5 mins is achieved, the oxygen concentration is increased. Although this method is not for real fire scenarios, it can be reproduced and does not depend on specimen thickness. Moreover, correlations to other flame retardancy tests, such as UL-94 and cone calorimeter [55] test, can be performed. LOI values read from the instrument correspond to the amount of oxygen a sample needs in order to burn consistently. The oxygen amount in atmospheric air is 21%, so any samples with LOI values lower than this tend to burn easily in the air. Samples with LOI values between 21% and 28% are considered to be "slow-burning". Samples with LOI values of 28% or higher are considered "self-extinguishing". Polyethylene, the most common polymer, has LOI value of 17% and burns easily. Rigid PVC has LOI value of around 40%. PTFE, one of the hardest polymers to burn, has LOI value of about 95%.

With this method, numerical values for LOI up to two significant figures can be measured. This can also lead to finding the effectiveness of synergism and antagonism of additives by measuring the deviation from standard values [17].

2.4.3 Scanning Electron Microscopy (SEM)

Scanning electron microscopy is an important tool for viewing of the surface of a specimen. Unlike normal microscopes, it uses electrons instead of light. By sending electrons to the surface and collecting the reflected or scattered electrons, the surface of the specimen can be analyzed with magnification up to 100000 on computer software. In addition, with energy dispersive x-ray (EDX) spectroscopy, elemental atom analyses can also be made to determine surface composition of samples. Surface coating is needed to make the surface conductive and this is achieved by high vacuum evaporation of gold or silver [56].

2.5 Previous Studies

Doğan et al. [57] studied the synergism of zinc phosphinate (ZnPi) and organo modified clay with PET fibers. They showed in their study that adding zinc phosphinate to PET fiber did not affect the flame retardant properties but decreased the mechanical properties. However, adding organoclay with ZnPi improved the flame retardant properties of PET fiber but decreased the mechanical properties further.

Vannier et al. [58] reported in their study that adding ZnPi resulted in intumescent property which improved the flame retardancy of PET. However, adding polyhedral oligomeric silsesquioxanes (POSS) contributed to the char strength of the material which indicated the synergistic effect between POSS and ZnPi. In a later study by the same scientists [59], this synergistic effect was found to be physical through the formation of an inorganic barrier.

Didane et al. [60] studied synergistic effect between different POSS structures and ZnPi on PET. Total heat evolved values (THE) decreased after adding ZnPi to PET. THE decreased further when any of these different POSS structures were added to PET together with ZnPi, improving the flame retardant properties of PET.

CHAPTER 3

EXPERIMENTAL WORK

3.1 Materials

PET with intrinsic viscosity of 0.600 dl/g was supplied by SASA, Adana Turkey. Zinc diethylphosphinate (zinc phosphinate, ZnPi) compound with trade name of Exolit OP950 was supplied by Clariant. The important characteristic of zinc phosphinate is that it is a liquid at the processing temperature of PET fiber and stable between the processing and melting temperature. Figure 3.1 shows the chemical formula of ZnPi compound. Properties of ZnPi are given in Table 3.1.

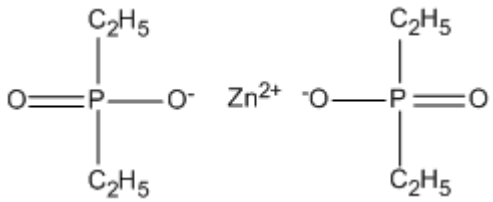

Figure 3.1 – Chemical formula of zinc phosphinate compound

Table 3.1 Properties of Exolit OP 950 [61]

Property	**Value**
Phosphorus content (%(w/w))	19.5-20.5
Moisture (%(w/w))	≤ 0.25
Density (g/cm^3)	1.3
Decomposition Temperature (°C)	≥ 350

Zinc borate ($2ZnO{\cdot}3B_2O_3{\cdot}3.5H_2O$) (ZnB) was kindly donated by ETI Mine Works. Huntite-hydromagnesite, trademarked as Ultracarb, was procured from Minelco. The reason for using huntite-hydromagnesite is that both huntite and hydromagnesite are minerals that can be found in Turkey and therefore can be obtained easily and cheap. Chemical composition and properties of huntite-hydromagnesite (HH) are given in Table 3.2 and 3.3, respectively.

Table 3.2 Chemical composition of huntite-hydromagnesite [62]

Chemical Analysis	**% weight**
MgO	36-39
CaO	6-9
SiO_2	0.2-1
Al_2O_3	0.1
SO_3	0.1
Fe_2O_3	0.05
K_2O	0.1
TiO_2	0.1

Table 3.3 Properties of huntite-hydromagnesite [62]

Property	**Value**
Specific gravity	2.5
Oil absorption	20-40g/100g
Refractive index	1.56
Surface area (m^2/g)	11-13
Hardness (Mohs)	2.5
Loose bulk density (kg/L)	0.2-0.5
Particle size (D_{50}) (μm)	3

Polyoxyethylene (20) sorbitan monopalmitate, trademarked as Tween 40 and a non-ionic surface active agent (oil soluble), which was used in surface treatment of zinc borate, was supplied by Merck.

3.2 Sample Preparation

3.2.1 Extrusion

PET fiber samples were prepared using a twin-screw micro compounder DSM Xplore (Figure 3.2). The processing conditions in the micro compounder were kept constant for each sample as mixing time of 3 minutes, screw speed of 100 rpm and processing temperature of 265 ℃. Specifications of the compounder can be seen in Table 3.4.

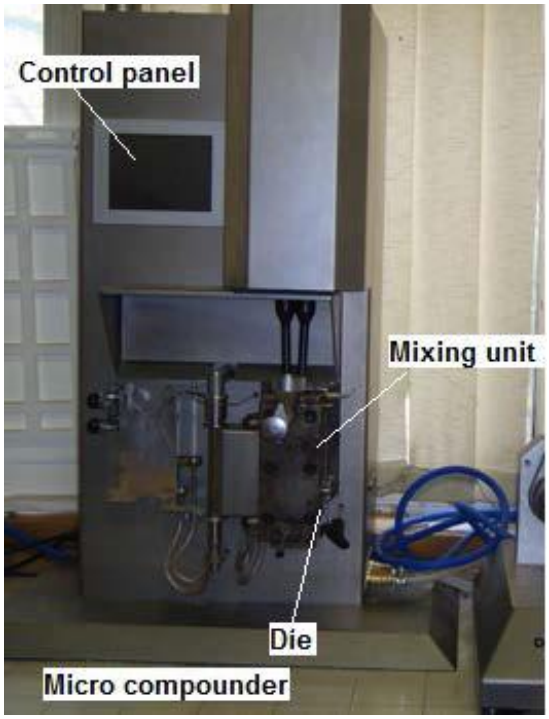

Figure 3.2 – Twin screw micro compounder (DSM Xplore)

Table 3.4 Specification of Xplore Micro-Compounder

Mixing/Dispersion control type	RPM or Axial Force
Maximum Axial Force	8000 N
Screw speed range	1-250 rpm
Hopper volume	15 mL
Maximum torque	10 N/m per screw

3.2.2 Drying

Drying process for main fiber samples and test samples were done using an oven with vacuum setup. The oven was set up to be at 100 ºC and 24 hour under vacuum (0.1 mbar).

3.2.3 Samples

Table 3.5 lists the PET samples percentages and labels that were prepared using zinc phosphinate (ZnPi), zinc borate (ZnB) and huntite-hydromagnesite (HH).

Table 3.5 –Percentages and labels of all PET samples that were prepared in this study

Label	ZnPi	ZnB	Treated-ZnB	Batch mixed-ZnB	HH	PET
OP0	-	-	-	-	-	100
OP5	5	-	-	-	-	95
OP10	10	-	-	-	-	90
OP15	15	-	-	-	-	85
OP20	20	-	-	-	-	80
OP10ZnB2	10	2	-	-	-	88
OP10T-ZnB2	10	-	2	-	-	88
OP10BM-ZnB2	10	-	-	2	-	88
OP10HH2	10	-	-	-	2	88
OP10HH4	10	-	-	-	4	86
OP0HH10	0	-	-	-	10	90

3.3 Tensile Tests

3.3.1 Standard Test Method for Tensile Properties of Plastics (ASTM D638-03)

In earlier part of the tests, ASTM D638-03 was used to determine the tensile properties of the samples obtained from the micro compounder. Tests were done under 5 kN load cell using a Lloyd tensile testing machine (Figure 3.3). The crosshead speed was 5 mm/min.

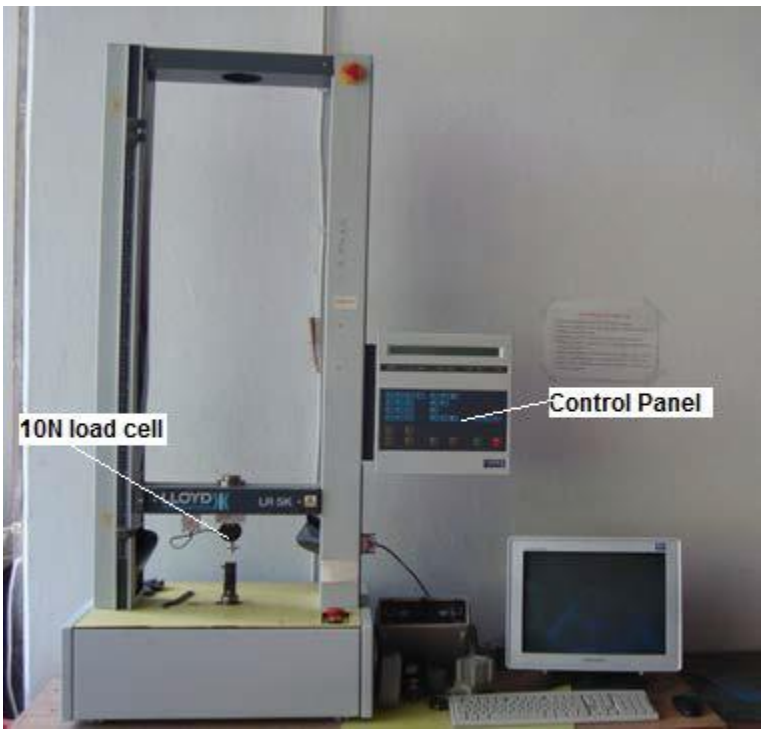

Figure 3.3 – Tensile testing machine (Lloyd)

Dog-bone samples were prepared using micro injection molding machine (Data Instruments) (Figure 3.4). Dimensions of the injected molded samples can be seen in Figures 3.5 and 3.6.

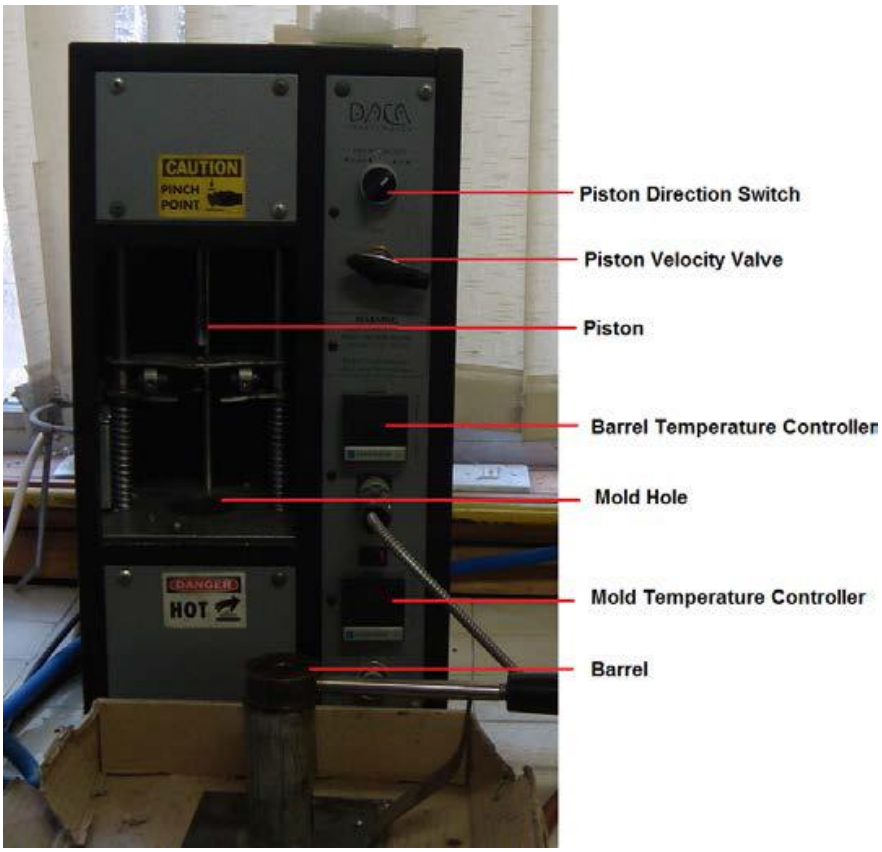

Figure 3.4 – Injection molding machine

Figure 3.5 – View of the dog-bone mold in the injection molding machine

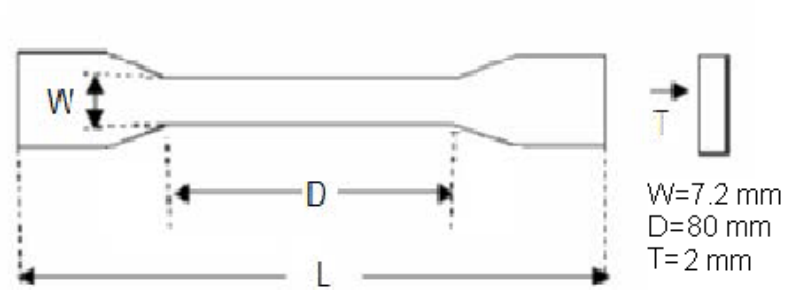

Figure 3.6 – Dimensions for dog-bone mold

Parameters for the preparation of mold were as follows: Nozzle temperatures of 250 ºC, mold temperature of 25 ºC, filling and holding times at 30 secs with 8 bar pressure.

For each set of experiment, average of three samples was taken and standard deviation values were recorded.

3.3.2 Standard Test Method for Tensile Strength and Young's Modulus of Fibers (ASTM C1557)

Mechanical properties for fiber samples were determined according to ASTM C1557 standard. Single fibers which were produced by micro compounder (Figure 3.2) were then drawn (draw ratio of 1:2 to 1:3) at 90 ºC with a drawing unit (Figure 3.7).

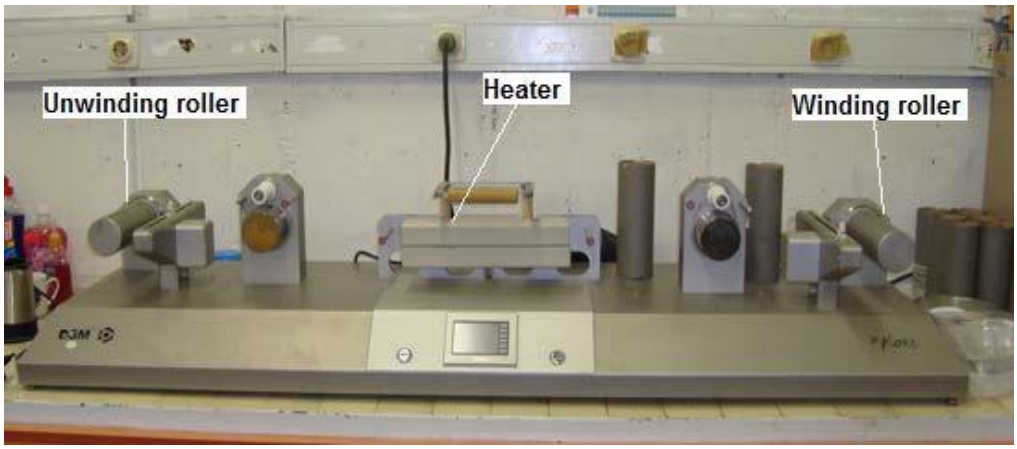

Figure 3.7 – DSM Xplore Microfiber spin line

The resulting diameters after drawing were measured by an 18 X Veho usb microscope. Tensile tests were repeated 10 times for each set of sample and standard deviation values were taken. The crosshead speed was 50 mm/min.

3.4 Flammability Tests

Flammability tests were done using a Limiting Oxygen Index (LOI) test apparatus (Fire Testing Technology) (Figure 3.8) according to ASTM D2863.

Figure 3.8 – Limiting oxygen index machine

The dimensions for the samples containing only ZnPi as an additive are shown in Figure 3.9. Samples were prepared using a compression molding machine (Figure 3.10) at 250 ºC and 3 min pressure application time.

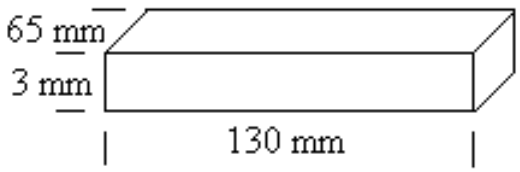

Figure 3.9 Dimensions for LOI test sample

Figure 3.10 Compression molding machine.

To measure the LOI values of the fibers, a loose fabric was produced. It is made by lining single fibers to resemble woven mat. A sample of 1 horizontal and 1 vertical layer is shown in Figure 3.11 and a total of 6 layers were prepared. Samples were then put into compression molding machine (Figure 3.10) at the same processing conditions described in the first part of the test, that is, at 250 ºC and 3 min pressure application time.

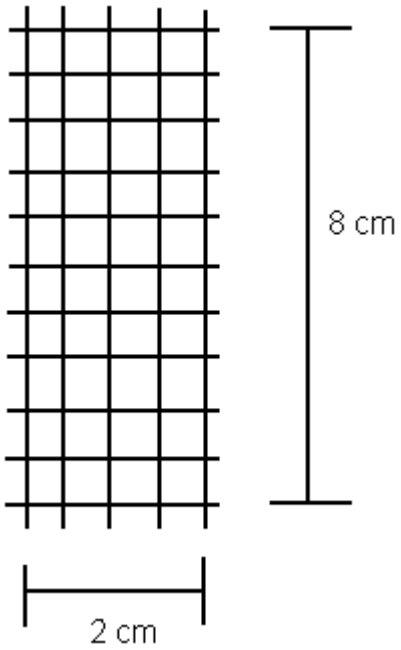

Figure 3.11 – Horizontal and vertical layers for woven-mat LOI sample

3.5 Wide Angle X-ray Scattering (WAXS)

X-ray diffraction for the fiber samples were done using a RIGAKU MiniFlex X-ray diffractometer at 30 kV/15 mA, with Cu radiation source. The scanning degree was from 2theta=5º to 40º with a step size of 0.1º.

3.6 Scanning Electron Microscopy (SEM) Analysis

Surfaces of fractured fiber samples were analyzed using a SEM machine, JEOL JSM-6400. Fractured surfaces were coated with gold and palladium mixture to provide the conductivity of the surface. Representative samples with good mechanical strength were observed with SEM. The elemental analysis of the surface was performed with Electron Dispersive X-ray spectroscopy (EDX).

CHAPTER 4

RESULTS AND DISCUSSION

4.1 Mechanical and Flame Retardant Properties

4.1.1 PET with Zinc Phosphinate (ZnPi)

As the first step in this work, the optimal amount of zinc phosphinate with respect to PET was taken into account. Table 4.1 gives the composition of the samples studied to optimize ZnPi amount in PET.

Table 4.1 – Samples with different percentages of Zinc phosphinate and PET

Label	Zinc Phosphinate (%)	PET (%)
OP0	0	100
OP5	5	95
OP10	10	90
OP15	15	85
OP20	20	80

By comparing the flame retardant properties and mechanical properties with respect to the percentage of zinc phosphinate used, an optimal zinc phosphinate amount can be obtained.

Figure 4.1 shows the mechanical behavior for different OP amounts in PET. Tensile tests with dog-bone shape samples were conducted.

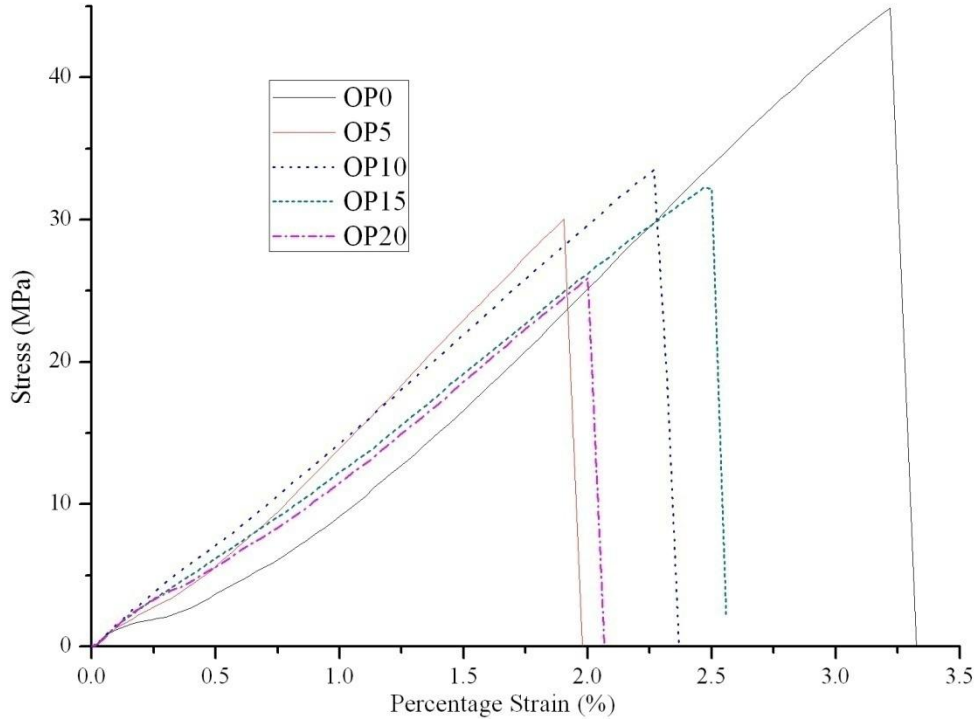

Figure 4.1 – Stress vs. strain of OP0, OP5, OP10, OP15, OP20

Table 4.2 shows the mechanical and flame retardant properties of the PET samples with different OP amounts.

Table 4.2 – Tensile strength, maximum elongation and LOI values for OP0, 5, 10, 15, 20

	Tensile Strength (MPa)	Elongation at Break (%)	Limiting Oxygen Index (% Oxygen)
OP0	46.9±5.6	3.2±0.5	25.5
OP5	31.0±6.2	2.0±0.3	26.9
OP10	33.5±4.7	2.6±0.3	30.3
OP15	32.6±8.3	2.8±0.4	33.3
OP20	25.6±4.1	1.8±0.6	37.1

OP10 seems like the best choice balancing the LOI and mechanical values due to highest tensile stress among PET samples with ZnPi and average LOI value. Therefore, in further tests, emphasis is given to 10% OP containing samples.

The effect of organo-phosphinate (ZnPi) on the morphology of PET is investigated by a series of wide-angle X-ray diffraction studies. The results of XRD experiments from sample OP0 to OP20 are given in Figure 4.2. For all samples, the basic diffraction pattern is the same. However, a very interesting observation is made for OP15 and OP20. A new structure is observed at 2theta = 9.18° and 11.7° for OP15 and 2theta = 9.28° and 11.8° for OP20. Furthermore, a small peak at 2theta = 32.98° for OP15 and 2theta = 32.86° for OP20 can be observed.

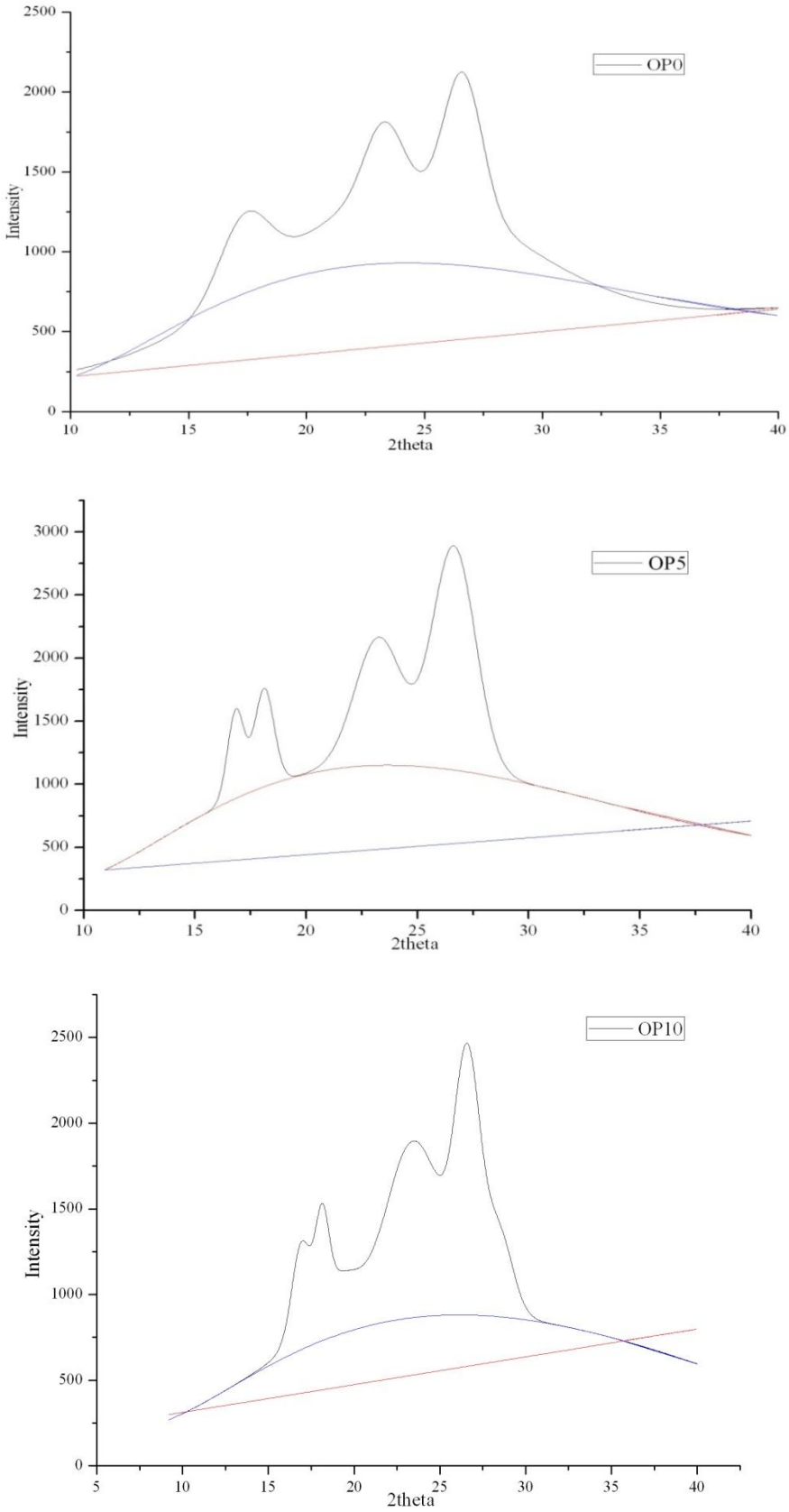

Figure 4.2 – WAXS intensity vs. 2theta for the samples OP0, OP5, OP10, OP15 and OP20 with baselines.

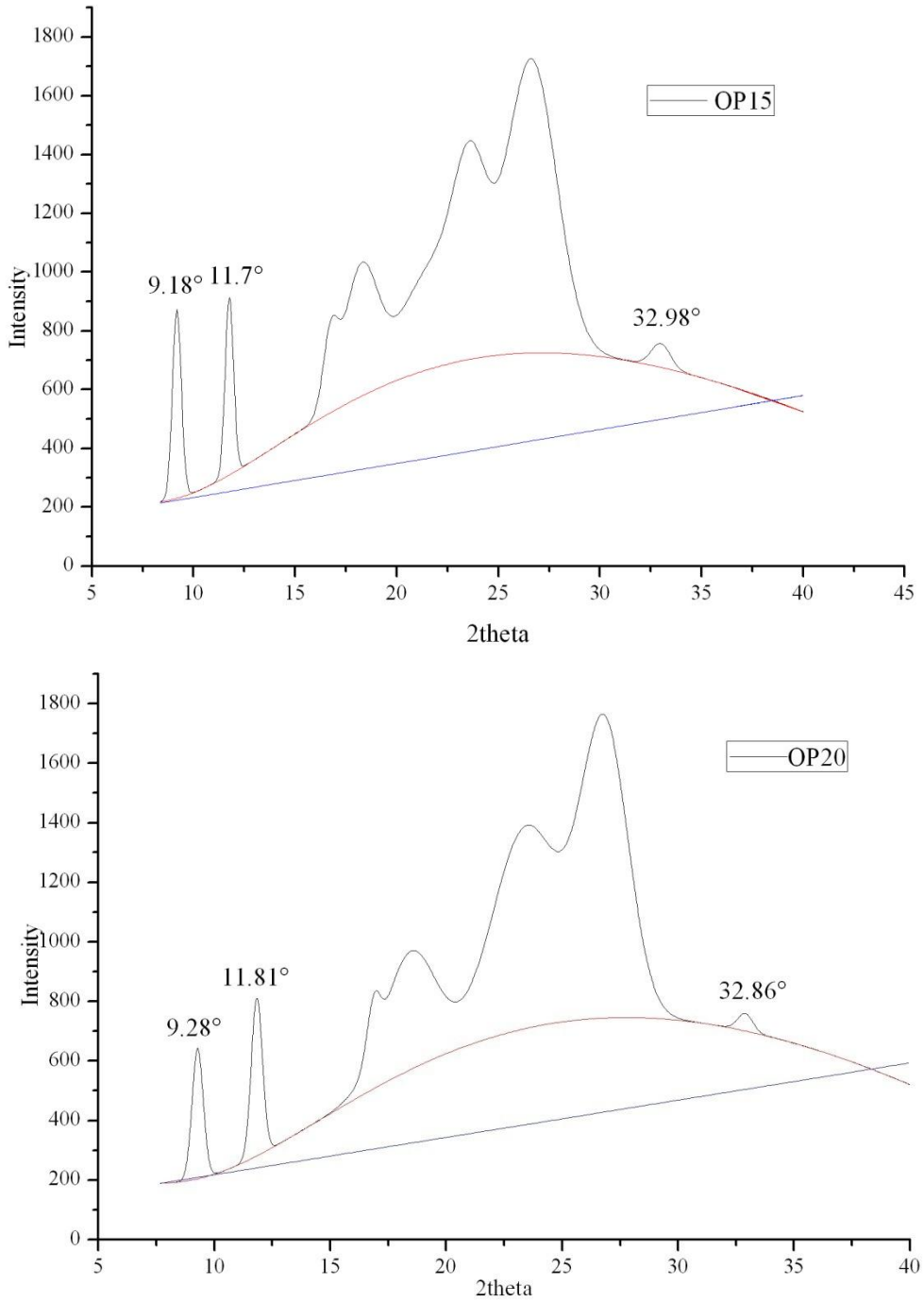

Figure 4.2 (cont'd) – WAXS intensity vs. 2theta for OP0, OP5, OP10, OP15, OP20, with baselines

These peaks do not exist at WAXS data of 5% and 10% OP. This means that ZnPi particles are absorbed completely and formed true solutions at these compositions. However, at 15% and 20% OP compositions, ZnPi particles start to form separate phases (phase separation). One phase is PET as a continuous phase; the other phase is ZnPi phase, as a discrete phase dispersed in continuous PET matrix.

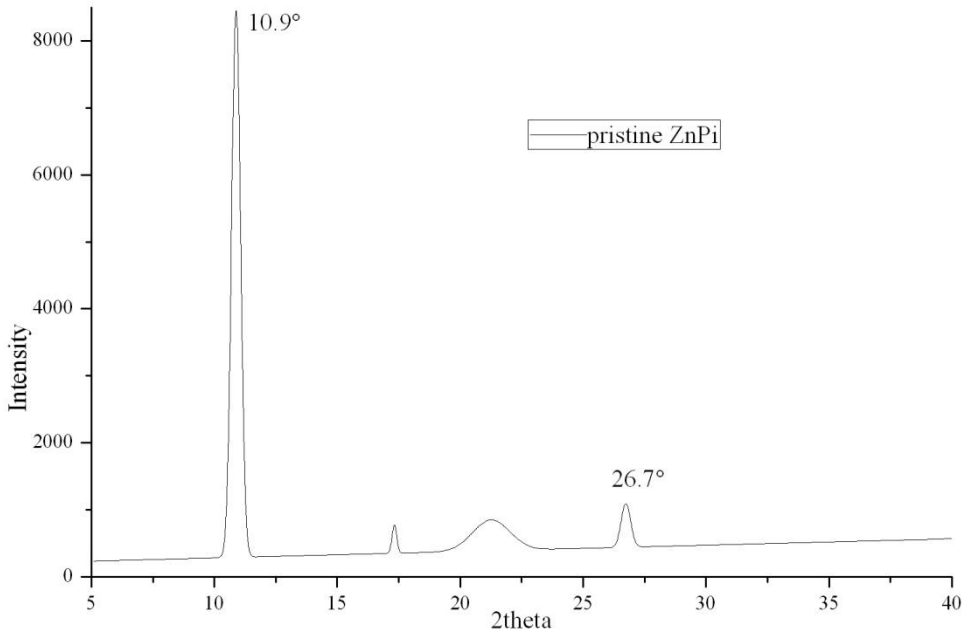

Figure 4.2a – WAXS intensity vs. 2theta graph of 100% ZnPi sample

To check this hypothesis, an XRD pattern of ZnPi is necessary to match newly formed peaks to the ZnPi crystal structure. Thus, we have performed WAXS on ZnPi (Figure 4.2a) and observed a very strong peak at around 2theta = 11° similar to the peak observed in the OP15 and OP20 samples. The other small peak at around 2theta = 33° for OP15 and OP20 is at lower (2theta = 26.7°) diffraction angles for pristine ZnPi. This difference in 2theta can be attributed to the colloidal nature of ZnPi in the PET continuous phase. There may be a change in crystal plane separations for surface atoms and the bulk atoms. This gives rise to two separate peaks for colloidal samples.

Our choice of 10% ZnPi addition to the remaining trials seems to be very appropriate regarding the maximum solubility of ZnPi in molten PET to form a homogeneous solution.

By looking at percent crystallinities of the OP15 and OP20 in Table 4.3, we can attribute their relatively high crystallinity to the crystal structure of phase separated ZnPi. ZnPi gives an additional material that can crystallize separately from PET. The low crystallinity of pure PET (OP0) is puzzling. Somehow the presence of ZnPi gives rise to more crystalline PET compared to pristine PET. WAXS is not the most correct instrument to measure crystallinities quantitavely.

Table 4.3 – Crystalline and amorphous area from the WAXS in Figure 4.2 and percent crystallinity

	Crystalline area	Amorphous area	Percent Crystallinity (%)
OP0	6953.5	23371.2	22.9
OP5	8662.9	27085.7	24.2
OP10	8991.3	23754.3	27.4
OP15	7318.5	18843.2	28.0
OP20	6814.6	18743.5	26.6

4.1.2 Zinc Borate as a Synergistic Agent

After deciding the ideal amount of OP, zinc borate is considered as the first synergist of the study to be used with OP. Zinc borate and zinc phosphinate may interact with each other to form a stronger char structure and give better flame retardant properties compared to ZnPi+PET samples. Table 4.4 shows the percentages of the PET samples prepared and labels used for these samples.

Table 4.4 – Samples with percentages of Zinc phosphinate, zinc borate and PET

Label	Zinc Phosphinate (%)	Zinc Borate (%)	PET (%)
OP0	0	0	100
OP10	10	0	90
OP10ZnB2	10	2	88

Until this point we made use of dog-bone shaped samples in our tensile measurements. However, fiber mechanical and flame retardant properties are the main concern. Therefore, ASTM C1557 was used for mechanical properties of fibers and for woven-mat samples ASTM D2863 was used to determine LOI values. The remaining fiber tests were performed on “Cold-Drawn” fiber to get better values. Draw ratios for zinc borate samples were as follows: 1:2.5 for OP0, 1:3.4 for OP10, 1:2 for OP10ZnB2.

Since 10% OP was the optimal amount, we decided to add 2% and 4% ZnB. However, in the case of 4% ZnB, tensile strength was so low that it was almost impossible to perform mechanical tests. Therefore, we decided to focus on 2% ZnB.

Figure 4.3 shows the stress-strain curves for OP0, OP10 and OP10ZnB2.

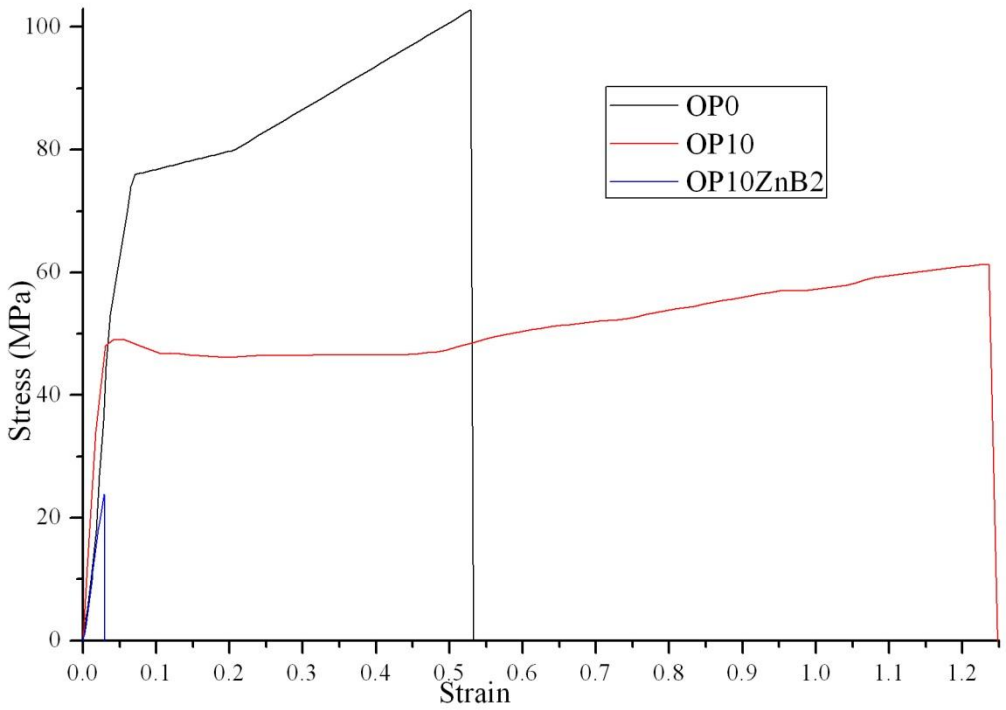

Figure 4.3 – Stress vs. Strain curve for OP0, OP10 and OP10ZnB2 fiber samples

Table 4.5 – Mechanical properties and LOI values for OP0, OP10, and OP10ZnB2

	Tensile Strength (MPa)	Elongation at break (%)	LOI (% Oxygen)
OP0	97.4±8.5	47.5±8.6	25.5
OP10	65.7±11.3	69.8±8.5	27
OP10ZnB2	23.3±5.4	3.3±0.5	29

From Table 4.5, LOI values after adding ZnB increase slightly and it confirms the consideration that it improves flame retardant properties of PET with OP. However, both tensile strength and elongation at break values are significantly lower compared to neat PET and OP10. This can be attributed to the agglomeration of ZnB particles in the PET fibers. When introducing ZnB into the PET through extrusion, ZnB particles clump together to give a poor dispersion in the fiber, forming agglomerates in the fiber and lowering the mechanical properties.

4.1.3 Adding Surface Treated Zinc Borate

To counteract agglomeration, surface treatment is needed. By performing surface treatment using a nonionic surfactant, which is polysorbate in this case, the interaction between nano-ZnB particles are minimized and therefore particles are expected to be dispersed. Two different ways for surface treatment were used. The first was to mix Tween 40 with nano-ZnB in a nonpolar solvent, chloroform, and then evaporating chloroform. However, since this would cause cost inefficiency and wastes, mixing both Tween and nano-ZnB during the extrusion process (batch mixing) was considered as the second way. Table 4.6 gives the percentages for PET, ZnPi and the two types of zinc borate, that is, treated zinc borate (T-ZnB) and batch mixed zinc borate (BM-ZnB).

Table 4.6 – Samples with percentages of PET, zinc phosphinate and the two types of zinc borate

Label	Zinc Phosphinate (%)	Treated Zinc Borate (%)	Batch mixed Zinc Borate (%)	PET (%)
OP10T-ZnB2	10	2	0	88
OP10BM-ZnB2	10	0	2	88

In Figure 4.4, stress vs. strain graph for the two different surface treated ZnB-PET samples (OP10T-ZnB2 and OP10BM-ZnB2) are added on to Figure 4.3 to give better visualization and comparison.

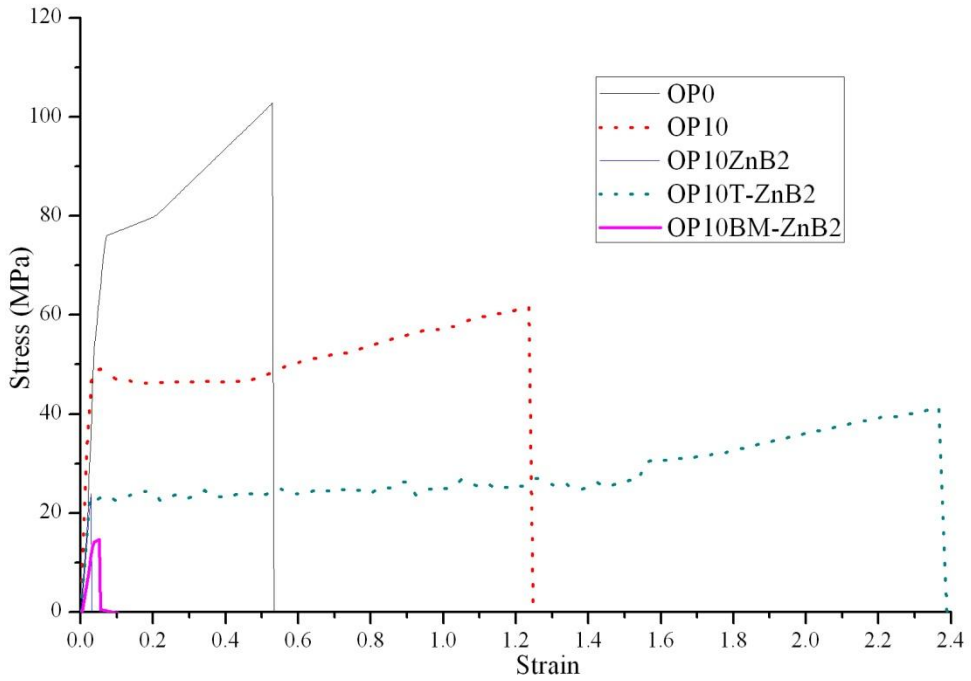

Figure 4.4 – Stress vs. strain curves for OP0, OP10, OP10ZnB2, OP10T-ZnB and OP10BM-ZnB2

ASTM C1557 was used for the mechanical tests for the samples with treated zinc borate. Draw ratios for treated zinc borate samples were as follows: 1:2 for OP10ZnB2, 1:2 for OP10T-ZnB2 and 1:3.5 for Op10BM-ZnB2. ASTM D2863 was used as the standard for determining the LOI values.

Table 4.7 – Mechanical and LOI values for surface treated nano-ZnB-PET fibers

	Tensile Strength (MPa)	Elongation at break (%)	LOI (% Oxygen)
OP0	97.4±8.5	47.5±8.6	25.5
OP10	65.7±11.3	69.8±8.5	27
OP10ZnB2	23.3±5.4	3.3±0.5	29
OP10T-ZnB2	29.5±9.3	217.9±35.1	32.1
OP10BM-ZnB2	14.0±4.5	6.6±2.8	32.4

It can be seen from Table 4.7 that applying surface treatment directly on nano-ZnB greatly improved mechanical properties, which supports the explanation that agglomeration was the cause for the poor mechanical properties obtained earlier. Moreover, good dispersion due to surface treatment also improved LOI values. On the other hand, batch mixing Tween and nano-ZnB in the micro compounder did not give the expected result, meaning that the method applied is not sufficient to prevent the agglomeration of ZnB particles.

However, in general zinc borate addition was detrimental to the mechanical properties with or without surface treatments. The tensile strengths are low but an interesting point is that the elongation at break value is extremely large (218%) for PET sample with 10% OP and 2% surface-treated zinc borate sample.

4.1.4 Huntite Hydromagnesite as a Synergist

As a next synergist, huntite-hydromagnesite is considered to be a good candidate. Upon decomposition, huntite-hydromagnesite releases water and CO_2 which will hamper flame occurrence and therefore improve flame retardancy. However, mechanical properties are also of importance here. If the synergism between huntite-hydromagnesite and zinc phosphinate does not exist, this may also lower the mechanical properties.

Samples containing 2% and 4% huntite-hydromagnesite with 10% OP were tested for mechanical and flame retardancy. As a further comparison, PET sample with 10% huntite-hydromagnesite and without zinc phosphinate was also tested to determine how effective huntite-hydromagnesite is in terms of flame retardancy and mechanical properties. Table 4.8 lists the percentages of PET, ZnPi and huntite-hydromagnesite. Figure 4.5 shows the stress vs. strain graphs of PET samples with ZnPi and huntite-hydromagnesite (OP10HH2 and OP10HH4) and PET sample with huntite-hydromagnesite only (OP0HH10).

Table 4.8 – Samples with percentages of PET, ZnPi and huntite-hydromagnesite

Label	Zinc Phosphinate (%)	Huntite-hydromagnesite (%)	PET (%)
OP10HH2	10	2	88
OP10HH4	10	4	86
OP0HH10	0	10	90

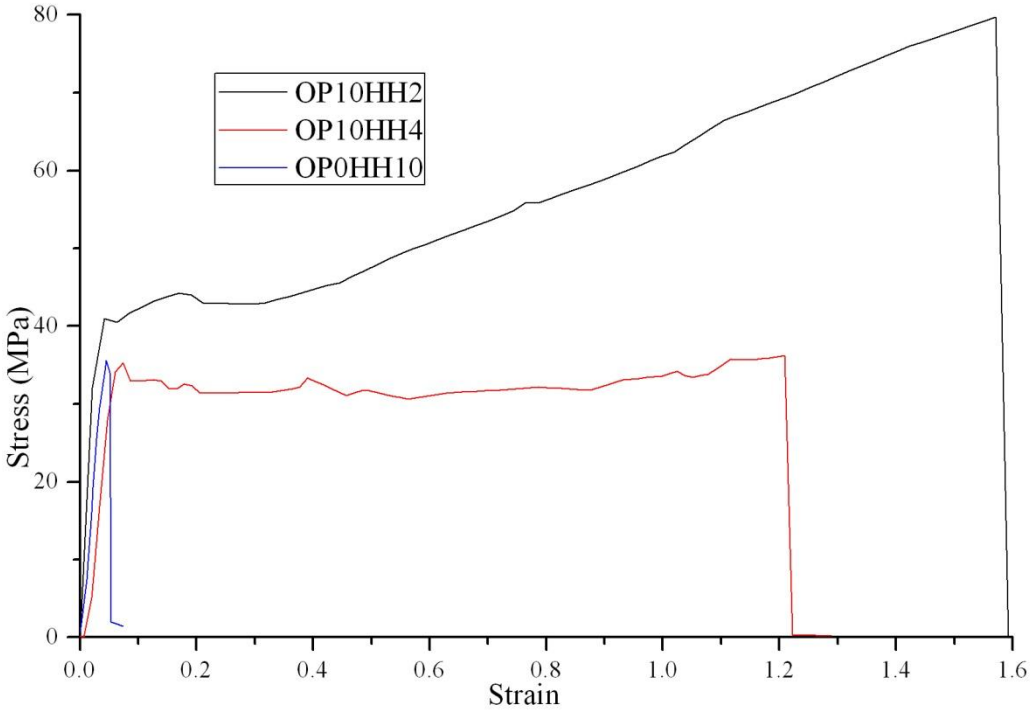

Figure 4.5 – Stress vs. strain curve for OP10HH2, OP10HH4 and OP0HH10 for fiber samples

ASTM C1557 was used for testing the mechanical properties of huntite-hydromagnesite samples. Cold drawing was done before the tests. Draw ratios for huntite-hydromagnesite samples were as follows: 1:2 for OP10HH2, 1:2 for OP10HH4, 1:1.85 for OP0HH10. To remember; the fibers used in these tests were subjected to cold-drawing at the above mentioned draw ratios before the tests.

Table 4.9 – Mechanical and LOI values of PET samples with both zinc phosphinate and huntite-hydromagnesite as the synergist

	Tensile Strength (MPa)	Elongation at break (%)	Limiting Oxygen Index (% Oxygen)
OP0	97.4±8.5	47.5±8.6	25.5
OP10	65.7±11.3	69.8±8.5	27
OP10ZnB2	23.3±5.4	3.3±0.5	29
OP10T-ZnB2	29.5±9.3	217.9±35.1	32.1
OP10BM-ZnB2	14.0±4.5	6.6±2.8	32.4
OP10HH2	75.0±13.1	161.4±30.9	30.5
OP10HH4	35.2±7.8	95.1±54.4	28.5
OP0HH10	32.3±5.9	4.7±1.0	20.3

As can be seen from Table 4.9, PET sample with 2% huntite-hydromagnesite has higher tensile strength than PET sample with 2% treated nano-ZnB. Elongation at break is also much larger than pure PET.

Comparing 4% huntite to 2% huntite, mechanical properties are lower and that is to be expected since more particles are introduced to the fiber. However, mechanical properties for huntite-hydromagnesite are lower than the other samples containing huntite-hydromagnesite. This means that there is a synergy between zinc phosphinate and huntite-hydromagnesite such that it improves the mechanical properties of huntite-hydromagnesite, ZnPi and PET system. This synergy exists for optimum 2% huntite containing samples.

Although there is a small decrease in LOI values for sample with 2% huntite compared to sample with 2% nano-ZnB, it is still better than pure PET or OP10. Moreover, sample with 4% huntite has lower LOI values than sample with 2% huntite, which is possible since PET sample with 10% huntite only has low LOI values and PET sample with 10% huntite cannot be regarded as a flame retardant for PET when used alone.

4.2 Morphological Analysis

Scanning electron microscopy (SEM) analyses were done to observe the fractured surfaces of PET samples with different synergist components. SEM images are presented with magnifications ranging from x500 to x2000. Fractures are formed by hand drawing and breaking of the fibers.

Figure 4.6a shows the fracture surface of a pristine PET sample. Fibril formations can be clearly seen on the fracture area. White areas are believed to be dust or other impurities. However, to the right of fracture, deformation areas can be observed. Figure 4.6b also shows another deformation area.

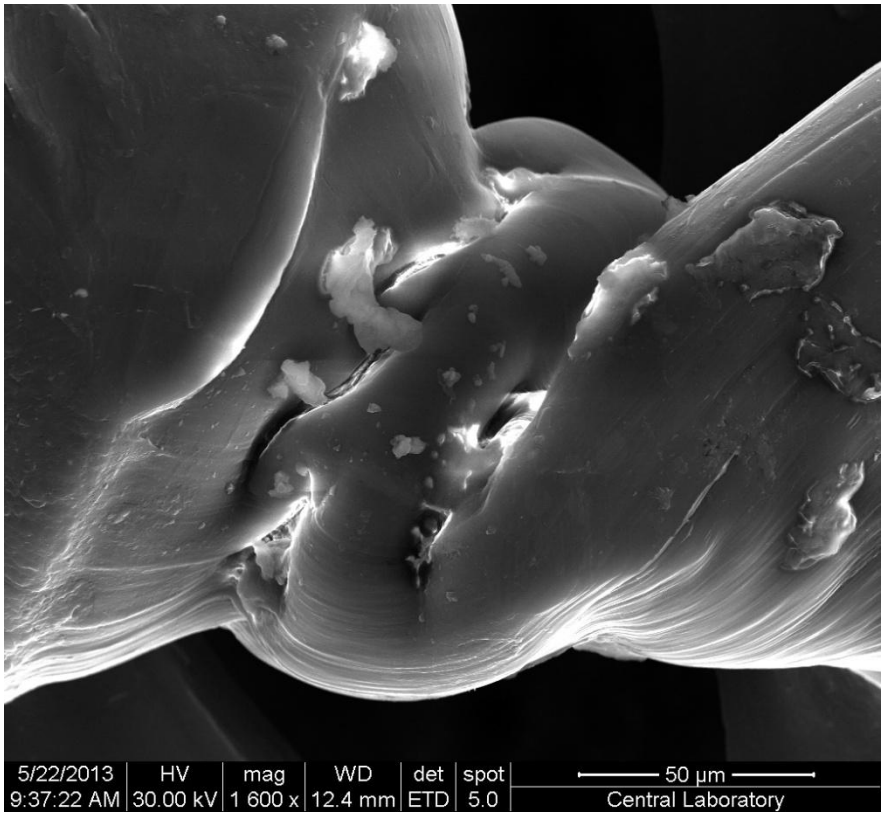

Figure 4.6a – SEM micrograph of a pure PET sample

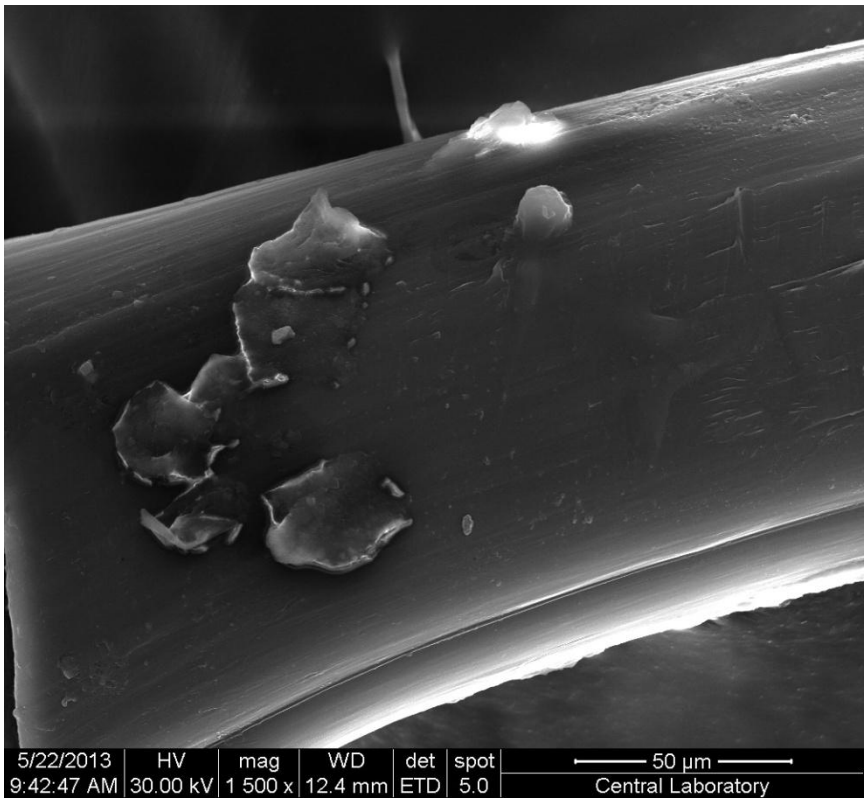

Figure 4.6b – SEM micrograph of PET showing the deformations on the surface

Figure 4.7a shows SEM micrograph of PET sample with 2% non-treated zinc borate and 10% ZnPi. Stretching and alignment can be seen on the middle of micrograph. Figure 4.7b shows a different area on the surface. Result of EDX analysis (Table 4.10) on the particle indicates that ZnPi, source of phosphorus element, isn't present as a separate phase. This means that dispersion on the surface is good, that is, ZnPi dissolves in the PET phase and zinc borate particles are coated with organic phase. Major constituents of the particle surface are C (67.5%), N (8.80%) and O (16.5%).

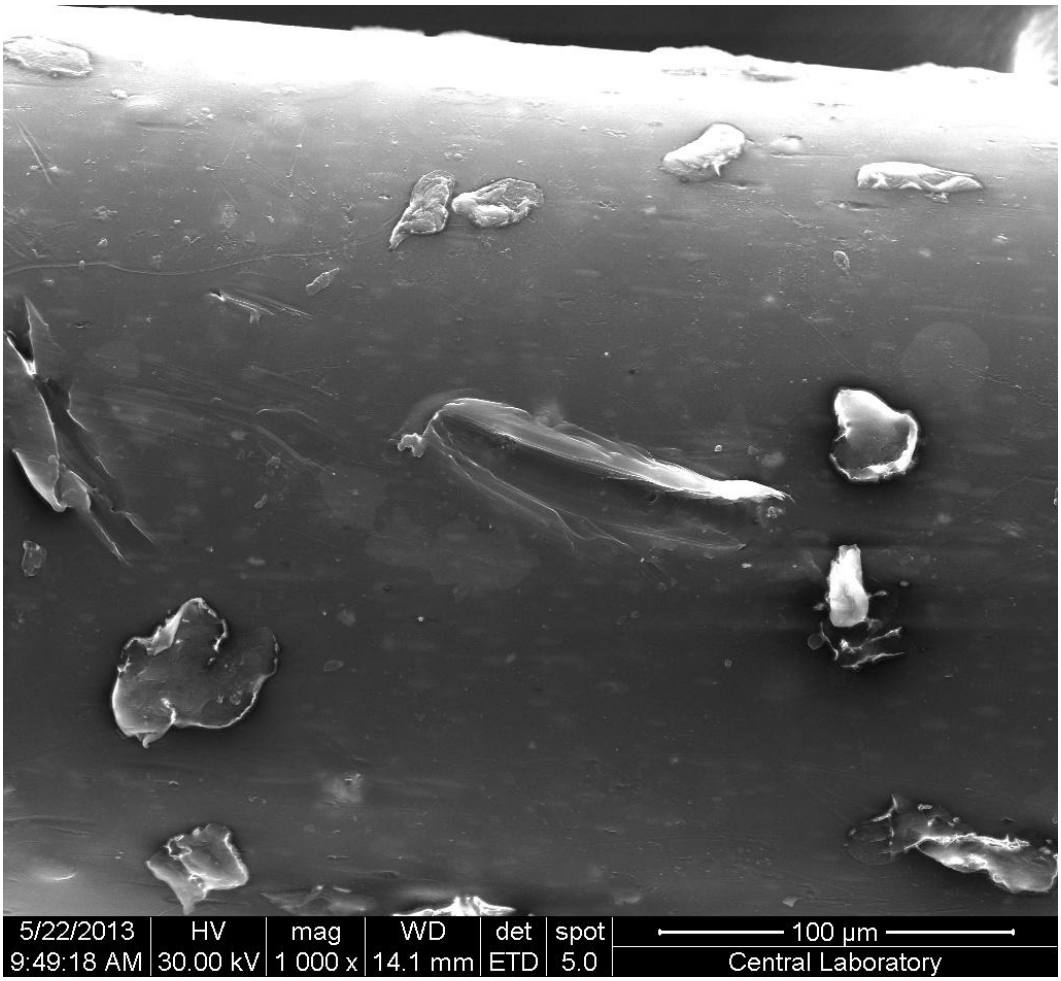

Figure 4.7a – SEM micrograph of PET with 2% ZnB and 10% ZnPi sample

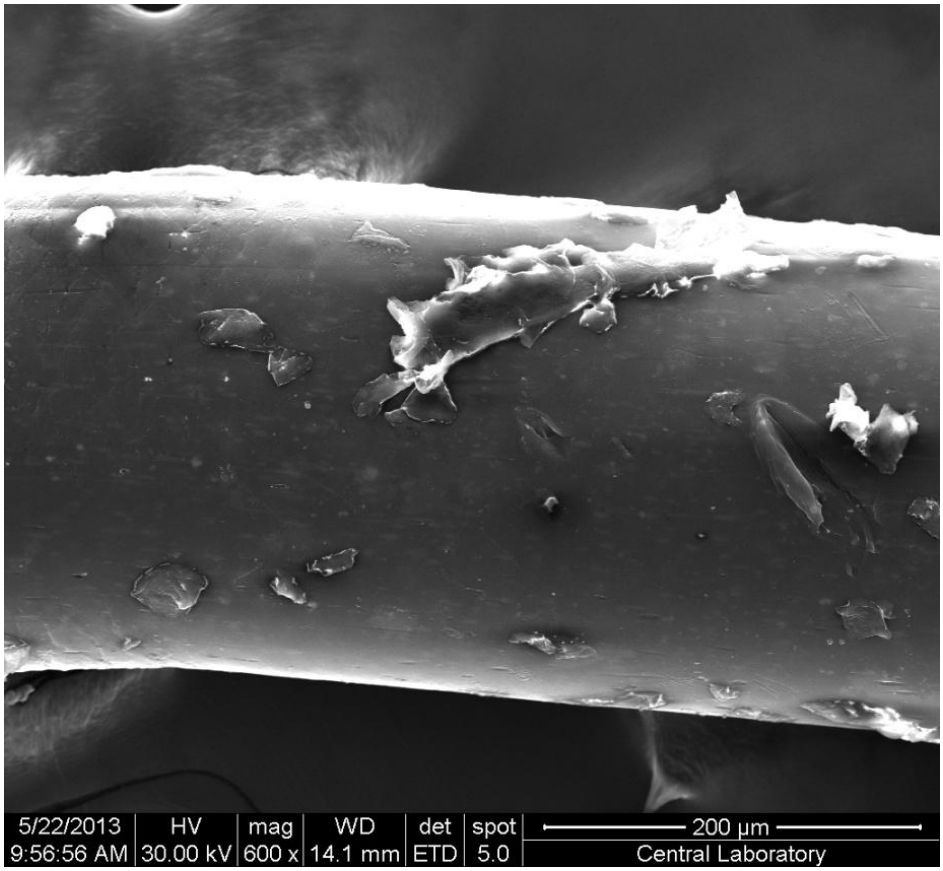

Figure 4.7b – SEM micrograph of the same PET sample with 2% ZnB and 10% ZnPi

Table 4.10 EDX analysis of the fiber surface of the PET sample 2% ZnB and 10% ZnPi

Element	Wt %	At %
C	67.49	75.77
N	8.80	8.47
O	16.48	13.89
Au	1.56	0.11
Mo	0.64	0.09
Cl	3.46	1.31
Pd	0.27	0.03
Ca	0.43	0.14
Zn	0.89	0.18
Total	100.00	100.00

Figure 4.8a shows the stretched area of PET sample with 2% surface-treated ZnB and 10% ZnPi. Fibrils and fracture pieces can be observed on the area. Figure 4.8b and Figure 4.8c show fractured ends of the sample. Again fibril formations can be seen. Table 4.11 gives the composition of elements on the stretch area. Zn percentage should be higher than phosphorus percentage since there are two Zn sources. This means that dispersion of additives is better than non-treated ZnB sample.

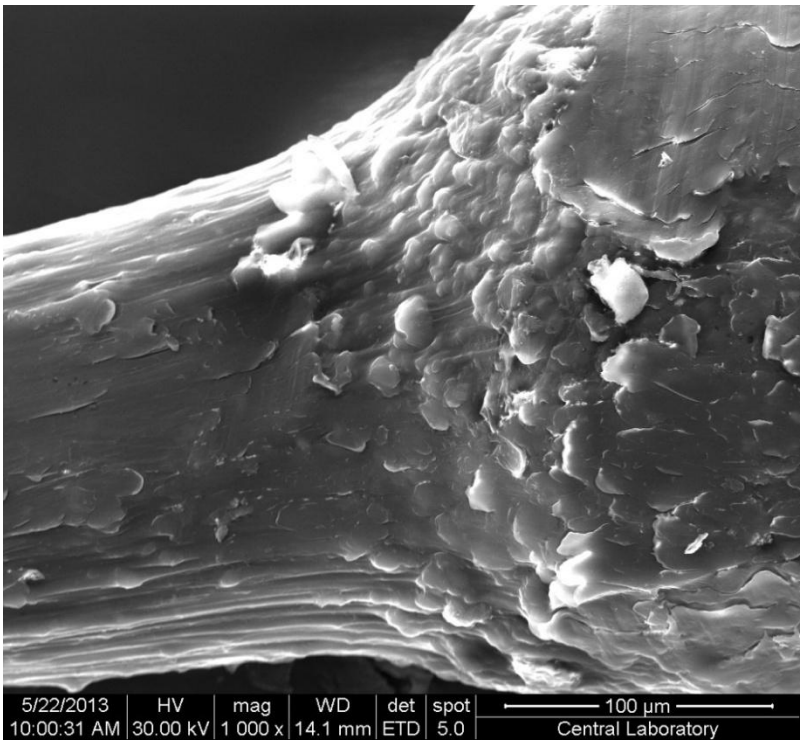

Figure 4.8a – SEM micrograph of stretch area of PET sample with 2% treated-ZnB and 10% ZnPi

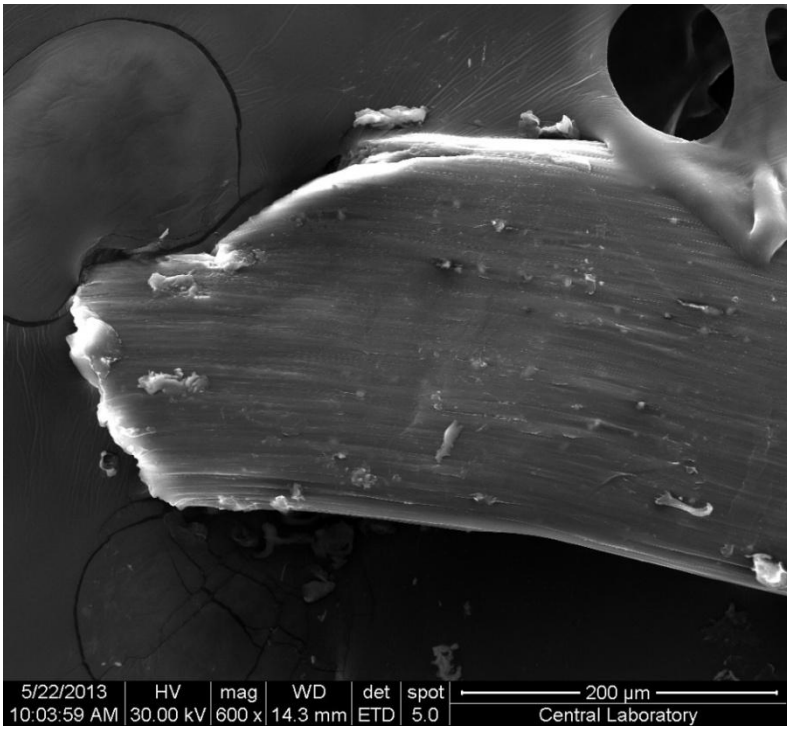

Figure 4.8b – SEM micrograph of fractured end of the same PET sample with 2% treated-ZnB and 10% ZnPi

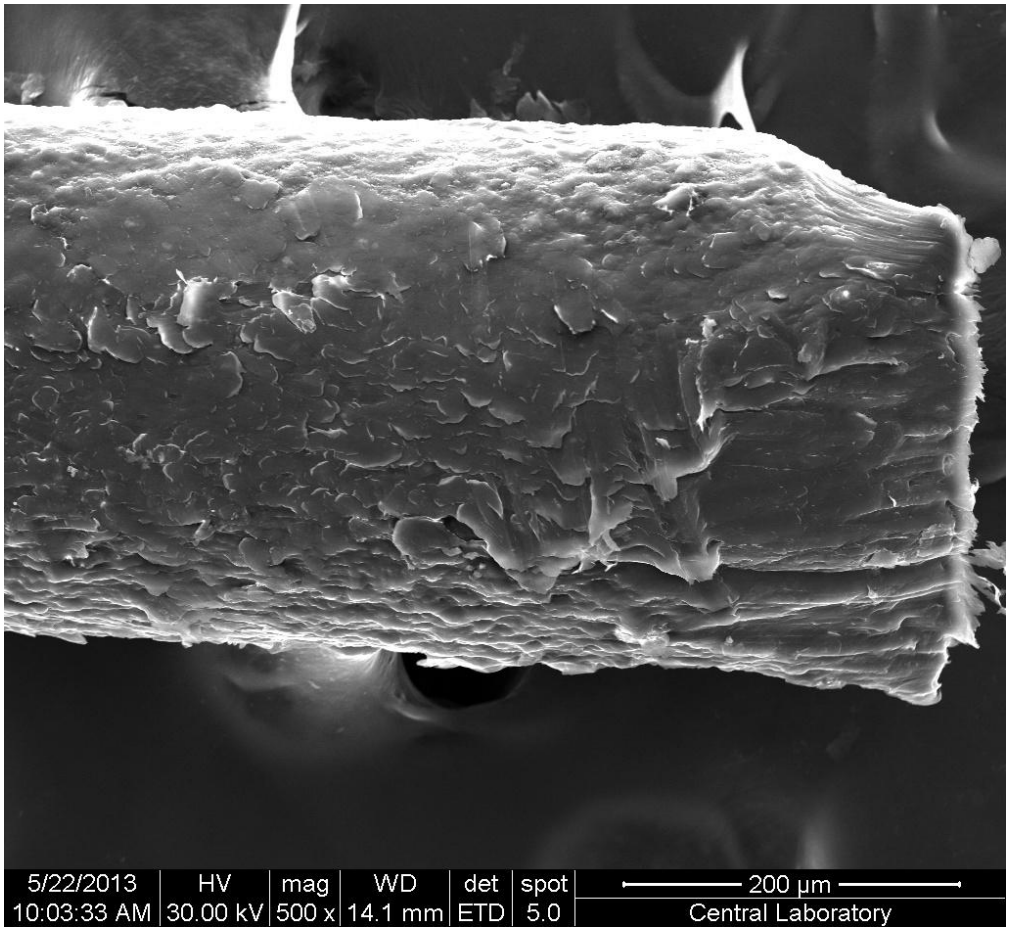

Figure 4.8C – SEM micrograph of the other end of the PET sample with 2% treated-ZnB and 10% ZnPi

Table 4.11 EDX analysis of the stretched area on PET sample with 2% treated-ZnB and 10% ZnPi

Element	Wt %	At %
C	77.58	84.06
O	18.27	14.86
P	1.15	0.48
Zn	3.01	0.60
Total	100.00	100.00

Figures 4.9a-4.9c show the SEM micrographs of PET sample with 2% huntite-hydromagnesite and 10% ZnPi. Figure 4.9a represents the alignment and therefore fibril formation on top portion of the photograph. Figure 4.9b shows one fractured end of the sample. It can be seen that fibril formation cannot be seen. However, fibril formations can be seen on the other end in Figure 4.9c. Table 4.12 shows the elemental analysis of the PET sample with 2% huntite-hydromagnesite and 10% ZnPi. Silicon source is SiO_2 present in the huntite-hydromagnesite. Amounts of both phosphorus and zinc indicate that there exists good dispersion on the surface.

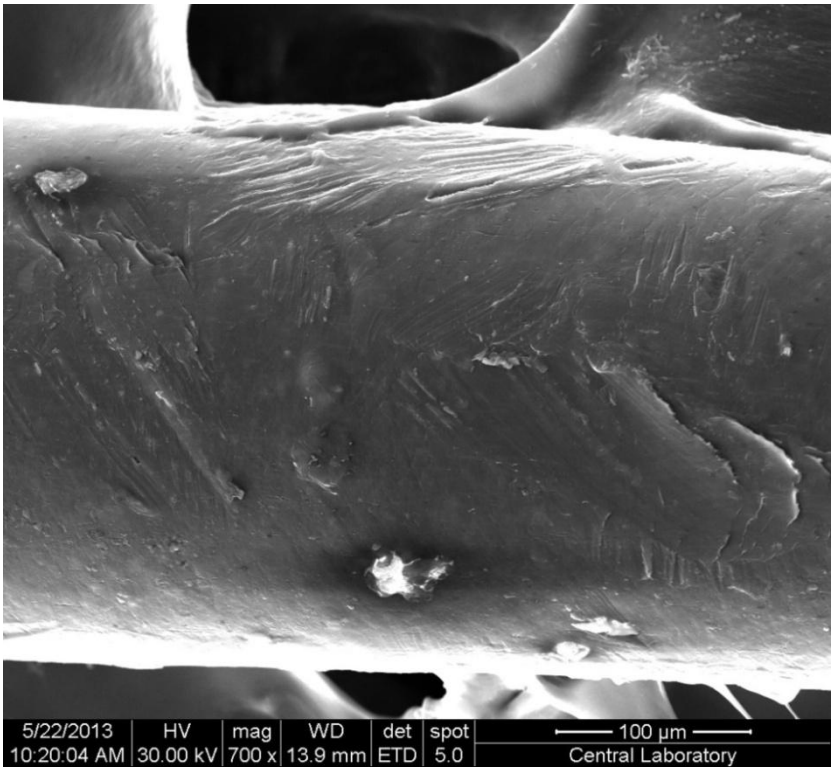

Figure 4.9a – SEM micrograph of PET sample with 2% huntite-hydromagnesite and 10% ZnPi

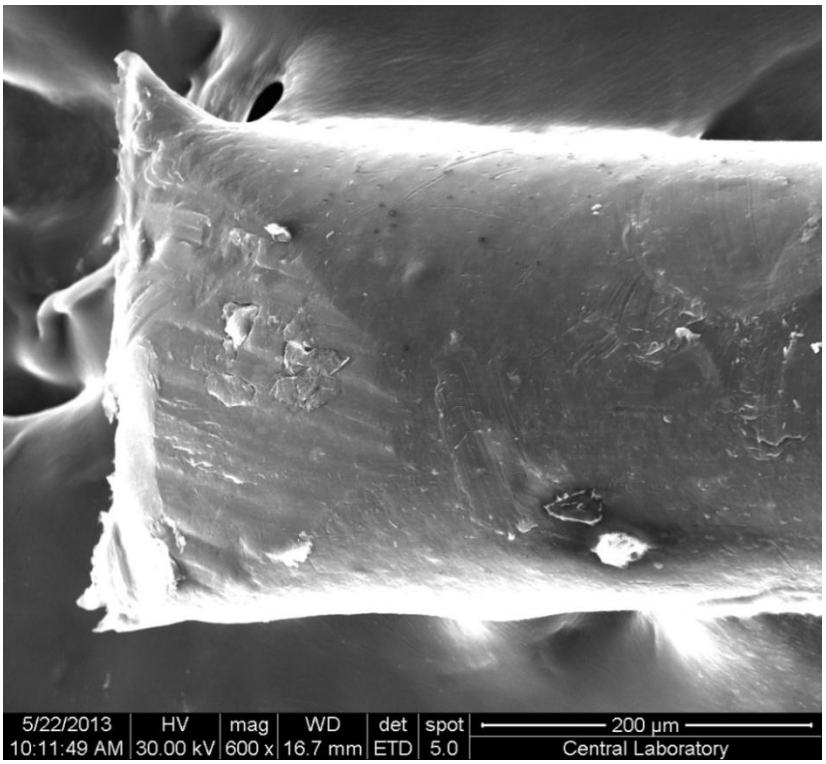

Figure 4.9b – One of the fractured ends of same PET sample with 2% huntite-hydromagnesite and 10% ZnPi

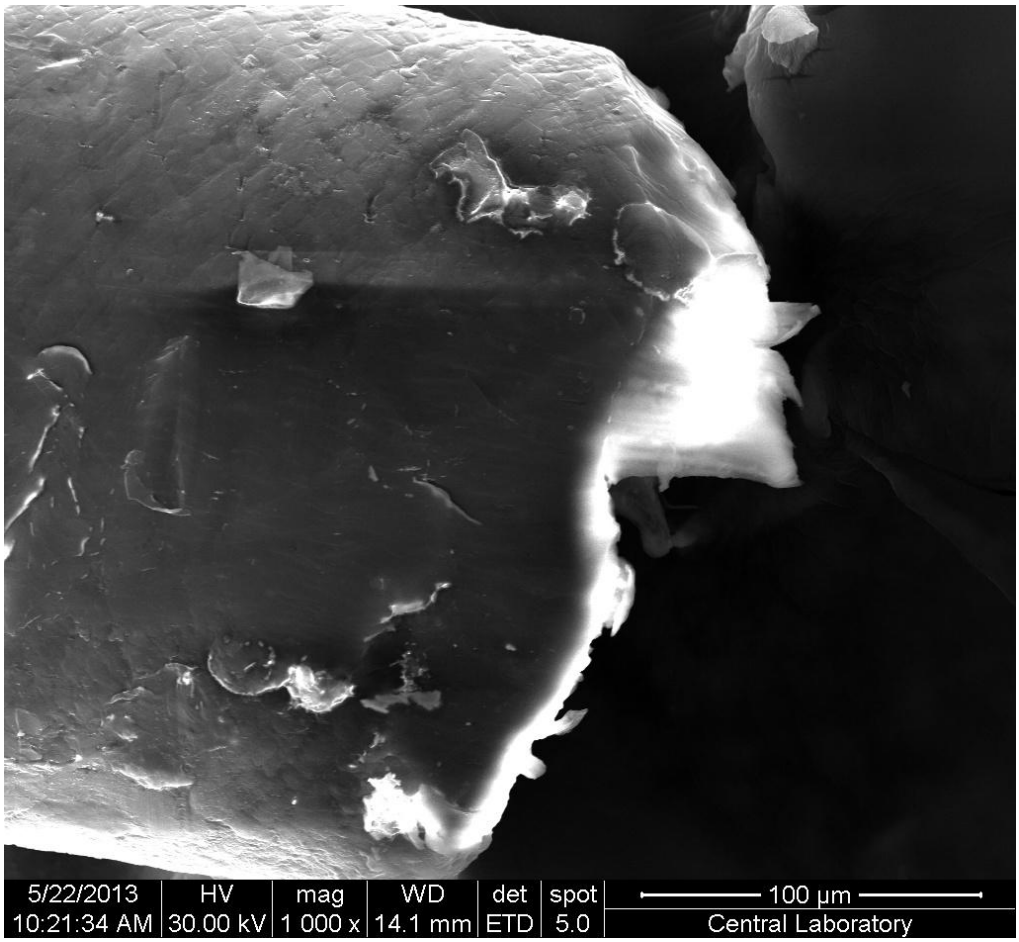

Figure 4.9c – The other fractured end of the PET sample with 2% huntite-hydromagnesite and 10% ZnPi

Table 4.12 EDX analysis of the PET sample with 2% huntite-hydromagnesite and 10% ZnPi

Element	Wt %	At %
C	78.08	83.90
O	18.81	15.18
Zn	1.74	0.34
Si	0.10	0.05
P	1.26	0.53
Total	100.00	100.00

CHAPTER 5

CONCLUSIONS

In this study, synergistic effects of different particles with zinc phosphinate on flame retardant and mechanical properties of PET-based systems were tested. First step was to find optimal amount of zinc phosphinate in terms of mechanical and flame retardant properties. From these, 10% ZnPi was found to be the optimum value. Also of importance is that at higher amounts of ZnPi phase separation between continuous phase PET and ZnPi discreet phase dispersed in PET phase was observed.

The first particle tested for synergy was nano-zinc borate since with zinc elements in both additives synergism may form easier. PET sample containing 2% zinc borate and 10% ZnPi exhibited good flame retardant property however its mechanical properties were quite low. Working on the assumption that agglomeration might be the cause, surface treatment to the zinc borate was applied. With this treatment, elongation at break was increased significantly but tensile strength remained low compared to pristine PET.

The second synergy agent was huntite-hydromagnesite since both huntite and hydromagnesite are minerals found in Turkey and may be a cost-reducing element in PET. Compared to zinc borate, PET with 2% huntite-hydromagnesite and 10% zinc phosphinate showed satisfactory flame retardant properties. Although elongation at break value was lower than that of ZnPi with zinc borate, which is not critical, it was still higher than pure PET. Tensile strength values were a little less than pristine PET and much better than PET samples containing zinc borate.

In conclusion, synergistic effect of both zinc borate and huntite-hydromagnesite were confirmed. Although zinc phosphinate with zinc borate provided good flame retardant properties, tensile strength value was low to be used as an additive for PET fibers. Zinc phosphinate with huntite-hydromagnesite, on the other hand, provided both good flame retardant properties and good mechanical properties so that they can be considered as synergistic additives in flame retardancy of PET fibers. Its fiber forming characteristic is also within acceptable limits as far as PET is concerned. In further work, surface modification by different surface active molecules can give rise to better synergy between huntite-hydromagnesite and zinc phosphinate.

REFERENCES

1. Ban, D. M., Y. Z. Wang, B. Yang, and G. M. Zhao, *A novel non-dripping oligomeric flame retardant for polyethylene terephthalate.* European Polymer Journal, 2004. **40**(8): p. 1909-1913.

2. Bednas, M.E., M. Day, K. Ho, R. Sander, and D.M. Wiles, *COMBUSTION AND PYROLYSIS OF POLY(ETHYLENE TEREPHTHALATE). - 1. THE ROLE OF FLAME RETARDANTS ON PRODUCTS OF PYROLYSIS.* Journal of Applied Polymer Science, 1981. **26**(1): p. 277-289.

3. Chen, D. Q., Y. Z. Wang, X. P. Hu, D. Y. Wang, M. H. Qu, and B. Yang, *Flame-retardant and anti-dripping effects of a novel char-forming flame retardant for the treatment of poly(ethylene terephthalate) fabrics.* Polymer Degradation and Stability, 2005. **88**(2): p. 349-356.

4. Koch, P.J., E.M. Pearce, J.A. Lapham, and S.W. Shalaby, *Flame-Retardant Poly(ethylene Terephthalate).* J. Appl. Polym. Sci., 1975. **19**: p. 227-234.

5. Laoutid, F., L. Ferry, J.M. Lopez-Cuesta, and A. Crespy, *Red phosphorus/aluminium oxide compositions as flame retardants in recycled poly(ethylene terephthalate).* Polymer Degradation and Stability, 2003. **82**(2): p. 357-363.

6. Lecomte, H.A. and J.J. Liggat, *Commercial fire-retarded PET formulations – Relationship between thermal degradation behaviour and fire-retardant action.* Polymer Degradation and Stability, 2008. **93**(2): p. 498-506.

7. Levchik, S.V. and E.D. Weil, *Flame retardancy of thermoplastic polyester - A review of the recent literature.* Polymer International, 2005. **54**(1): p. 11-35.

8. Bourbigot, S. and S. Duquesne, *Fire retardant polymers: recent developments and opportunities.* Journal of Materials Chemistry, 2007. **17**(22): p. 2283-2300.

9. Didane, N., S. Giraud, E. Devaux, G. Lemort, and G. Capon, *Thermal and fire resistance of fibrous materials made by PET containing flame retardant agents.* Polymer Degradation and Stability, 2012. **97**(12): p. 2545-2551.

10. Sato, M., S. Endo, Y. Araki, G.O. Matsuoka, S. Gyobu, and H. Takeuchi, *The flame-retardant polyester fiber: Improvement of hydrolysis resistance.* Journal of Applied Polymer Science, 2000. **78**(5): p. 1134-1138.

11. Wu, B., Y. Z. Wang, X. L. Wang, K. K. Yang, Y. D. Jin, and H. Zhao, *Kinetics of thermal oxidative degradation of phosphorus-containing flame retardant copolyesters.* Polymer Degradation and Stability, 2002. **76**(3): p. 401-409.

12. Zhao, H., Y. Z. Wang, D. Y. Wang, B. Wu, D. Q. Chen, X. L. Wang, and K. K. Yang, *Kinetics of thermal degradation of flame retardant copolyesters containing phosphorus linked pendent groups.* Polymer Degradation and Stability, 2003. **80**(1): p. 135-140.

13. Ou, C.F., M.T. Ho, and J.R. Lin, *Synthesis and characterization of poly(ethylene terephthalate) nanocomposites with organoclay.* Journal of Applied Polymer Science, 2004. **91**(1): p. 140-145.

14. Du, X. H., C. S. Zhao, Y. Z. Wang, Q. Zhou, Y. Deng, M. H. Qu, and B. Yang, *Thermal oxidative degradation behaviours of flame-retardant thermotropic liquid crystal copolyester/PET blends.* Materials Chemistry and Physics, 2006. **98**(1): p. 172-177.

15. Sain, M., S.H. Park, F. Suhara, and S. Law, *Flame retardant and mechanical properties of natural fibre–PP composites containing magnesium hydroxide.* Polymer Degradation and Stability, 2004. **83**(2): p. 363-367.

16. Zhang, Z.X., J. Zhang, B. X. Lu, Z.X. Xin, C.K. Kang, and J.K. Kim, *Effect of flame retardants on mechanical properties, flammability and foamability of PP/wood–fiber composites.* Composites Part B: Engineering, 2012. **43**(2): p. 150-158.

17. Weil, E.D. and S.V. Levchik, *Flame Retardants for Plastics and Textiles*, in *Flame Retardants*. 2009, Hanser. p. 248-250.

18. Grand, A.F. and C.A. Wilkie, *Fire retardancy of polymeric materials / edited by Arthur F. Grand, Charles A. Wilkie*. 2000: New York : Marcel Dekker, c2000.

19. Shaw, S.D., A. Blum, R. Weber, K. Kannan, D. Rich, D. Lucas, C.P. Koshland, D. Dobraca, S. Hanson, and L.S. Birnbaum, *Halogenated flame retardants: do the fire safety benefits justify the risks?* Rev Environ Health, 2010. **25**(4): p. 261-305.

20. Levchik, S.V. and E.D. Weil, *A Review of Recent Progress in Phosphorus-based Flame Retardants.* Journal of Fire Sciences, 2006. **24**(5): p. 345-364.

21. Zhao, C. S., F. L. Huang, W. C. Xiong, and Y. Z. Wang, *A novel halogen-free flame retardant for glass-fiber-reinforced poly(ethylene terephthalate).* Polymer Degradation and Stability, 2008. **93**(6): p. 1188-1193.

22. Işıtman, N.A. and C. Kaynak, *Flame retardancy of polymer nanocomposites [Electronic resource]/ Nihat Ali Işıtman, Supervisor Prof. Dr. Cevdet Kaynak*. Ankara : METU, 2012.

23. Laoutid, F., L. Bonnaud, M. Alexandre, J.M. Lopez-Cuesta, and P. Dubois, *New prospects in flame retardant polymer materials: From fundamentals to nanocomposites.* Materials Science and Engineering: R: Reports, 2009. **63**(3): p. 100-125.

24. Bourbigot, S., T. Turf, S. Bellayer, and S. Duquesne, *Polyhedral oligomeric silsesquioxane as flame retardant for thermoplastic polyurethane.* Polymer Degradation and Stability, 2009. **94**(8): p. 1230-1237.

25. Devaux, E., M. Rochery, and S. Bourbigot, *Polyurethane/clay and polyurethane/POSS nanocomposites as flame retarded coating for polyester and cotton fabrics.* Fire and Materials, 2002. **26**(4-5): p. 149-154.

26. Bourbigot, S., M. Le Bras, X. Flambard, M. Rochery, E. Devaux, and J.D. Lichtenhan, Polyhedral Oligomeric Silsesquioxanes: Applications to Flame Retardant Textiles, 2005: p. 189-201.

27. Fina, A., H.C.L. Abbenhuis, D. Tabuani, and G. Camino, *Metal functionalized POSS as fire retardants in polypropylene.* Polymer Degradation and Stability, 2006. **91**(10): p. 2275-2281.

28. Kashiwagi, T., R.H. Harris Jr, X. Zhang, R.M. Briber, B.H. Cipriano, S.R. Raghavan, W.H. Awad, and J.R. Shields, *Flame retardant mechanism of polyamide 6-clay nanocomposites.* Polymer, 2004. **45**(3): p. 881-891.

29. Hollingbery, L.A. and T.R. Hull, *The fire retardant behaviour of huntite and hydromagnesite – A review.* Polymer Degradation and Stability, 2010. **95**(12): p. 2213-2225.

30. Prokhorov, A.M., *Great Soviet encyclopedia*. Great Soviet Encyclopédia. 1982: Macmillan.

31. van der Vegt, A.K. and L.E. Govaert, *Polymeren: van keten tot kunststof*. 2005: Centraal Boekhuis.

32. E176-13, A.S., *Standard Terminology of Fire Standards*. April 2013, ASTM International, West Conshohocken, PA, 2003.

33. Andrae, N.J., *Durable and Environmentally Friendly Flame Retardants for Synthetics.* 2008.

34. Lewin, M. and S.B. Sello, *Handbook of Fiber Science and Technology: Functional Finishes. Chemical processing of fibers and fabrics. Volume II. Part A-B*. Chemical Processing of Fibers and Fabrics: Functional Finishes. 1984: Marcel Dekker.

35. Zhang, S. and A.R. Horrocks, *A review of flame retardant polypropylene fibres.* Progress in Polymer Science, 2003. **28**(11): p. 1517-1538.

36. D Weil, E., *Mechanisms and modes of action in flame retardancy of polymers.* Fire retardant materials, 2001: p. 31.

37. Dufton, P.W., *Flame Retardants for Plastics Market Report*. 2003: Rapra Technology Limited.

38. van der Veen, I. and J. de Boer, *Phosphorus flame retardants: Properties, production, environmental occurrence, toxicity and analysis.* Chemosphere, 2012. **88**(10): p. 1119-1153.

39. Cefic. *What are FRs? Flame Retardant Market Statistics*. 2006 08.07.2013]; Available from: http://www.cefic-efra.com/.

40. Kılınç, M. and G.Bayram, *Production and characterization of boron-based additives and the effect of flame retardant additives on pet-based composites [Electronic resource] / Mert Kılınç, Supervisor Assoc. Prof. Dr. Göknur Bayram*. Ankara : METU ; 2009.

41. Baltacı, B. and G. Bayram, *Sytnhesis and characterization of nano zinc borate and its usage as a flame retardant for polymers [Electronic resource] / Berk Baltacı, Supervisor Prof. Dr. Göknur Bayram*. Ankara : METU ; 2010.

42. Hshieh, F. Y., *Shielding effects of silica-ash layer on the combustion of silicones and their possible applications on the fire retardancy of organic polymers.* Fire and Materials, 1998. **22**(2): p. 69-76.

43. Weil, E.D., *Improved Fire- and Smoke-Resistant Materials for Commercial Aircraft Interiors:A Proceedings*. 1995: The National Academies Press.

44. Kangal, O., A.A. Sirkeci, and A. Güney, *Flotation behaviour of huntite (Mg3Ca(CO3)4) with anionic collectors.* International Journal of Mineral Processing, 2005. **75**(1–2): p. 31-39.

45. Ozao, R. and R. Otsuka, *Thermoanalytical investigation of huntite.* Thermochimica Acta, 1985. **86**(0): p. 45-58.

46. Kangal, O. and A. Güney, *A new industrial mineral: Huntite and its recovery.* Minerals Engineering, 2006. **19**(4): p. 376-378.

47. Barbieri, M., G. Calderoni, C. Cortesi, and M. Fornaseri, *HUNTITE, A MINERAL USED IN ANTIQUITY.* Archaeometry, 1974. **16**(2): p. 211-220.

48. Sawada, Y., K. Uematsu, N. Mizutani, and M. Kato, *Thermal decomposition of hydromagnesite 4MgCO3·Mg(OH)2·4H2O.* Journal of Inorganic and Nuclear Chemistry, 1978. **40**(6): p. 979-982.

49. Wyld, O., *British Patent 551*. 1735.

50. Horrocks, A.R., *Developments in flame retardants for heat and fire resistant textiles—the role of char formation and intumescence.* Polymer Degradation and Stability, 1996. **54**(2–3): p. 143-154.

51. Horrocks, A.R., *Textiles.* Fire retardant materials, 2001: p. 128.

52. Hastie, J.W.M., C. L. , *Mechanistic Studies of Triphenylphosphine Oxide-Poly(Ethylene-terephthalate) and Related Flame Retardant Systems. Final Report.* NBSIR 75-741, August 1975.

53. Shah, V., *Handbook of plastics testing technology*. 2nd ed. 1998: New York, NY (United States); John Wiley and Sons.

54. Kılınç, M. and G. Bayram, *Processing and characterization of poly(ethylene terephthalate) based composites [Electronic resource] / Mert Kılınç, supervisor Assoc. Prof. Dr. Göknur Bayram*. 2004: Ankara : METU ; 2004.

55. Weil, E.D., M.M. Hirschler, N.G. Patel, M.M. Said, and S. Shakir, *Oxygen index: Correlations to other fire tests.* Fire and Materials, 1992. **16**(4): p. 159-167.

56. Scheirs, J., *Compositional and failure analysis of polymers: a practical approach / John Scheirs*. 2000: New York : Wiley, 2000.

57. Doğan, M., S. Erdoğan, and E. Bayramlı, *Mechanical, thermal, and fire retardant properties of poly(ethylene terephthalate) fiber containing zinc phosphinate and organo-modified clay.* Journal of Thermal Analysis & Calorimetry, 2013. **112**(2): p. 871-876.

58. Vannier, A., S. Duquesne, S. Bourbigot, A. Castrovinci, G. Camino, and R. Delobel, *The use of POSS as synergist in intumescent recycled poly(ethylene terephthalate).* Polymer Degradation and Stability, 2008. **93**(4): p. 818-826.

59. Vannier, A., S. Duquesne, S. Bourbigot, J. Alongi, G. Camino, and R. Delobel, *Investigation of the thermal degradation of PET, zinc phosphinate, OMPOSS and their blends—Identification of the formed species.* Thermochimica Acta, 2009. **495**(1–2): p. 155-166.

60. Didane, N., S. Giraud, E. Devaux, and G. Lemort, *A comparative study of POSS as synergists with zinc phosphinates for PET fire retardancy.* Polymer Degradation and Stability, 2012. **97**(3): p. 383-391.

61. Clariant. *Exolit OP 950 Product Data Sheet*. 19.07.2012; Available from: http://www.additives.clariant.com/bu/additives/PDS_Additives.nsf/www/DS-FKON-8VQAET?open, last accessed on 11.07.2013.

62. Minelco. *Ultracarb Product Information*; Available from: http://www.quimexsudamericana.com.ar/ultracarb.pdf, last accessed on 01.07.2013.